Journal of Radiation Research and Applied Sciences 19 (2026) 102432

Contents lists available at ScienceDirect

Journal of Radiation Research and Applied Sciences

journal homepage: www.journals.elsevier.com/journal-of-radiation-research-and-applied-sciences

Development of the new beta Prime-G family of distributions for advanced modeling of radiation data

Ahmad Abubakar Suleiman [a,*], Zahrah Fayez Althobaiti [b], Hanita Daud [c], Nazreen Waeleh [d], Maysaa Elmahi Abd Elwahab [e], Raga Idress [f]

[a] Department of Statistics, Aliko Dangote University of Science and Technology, Wudil, 713281, Nigeria
[b] Department of Statistics, Faculty of Science, University of Tabuk, 71491, Tabuk, Saudi Arabia
[c] Department of Applied Science, Universiti Teknologi PETRONAS, Seri Iskandar, 32610, Malaysia
[d] Faculty of Electronics and Computer Technology and Engineering, Universiti Teknikal Malaysia Melaka (UTeM), 76100, Durian Tunggal, Melaka, Malaysia
[e] Department of Mathematical Sciences, College of Science, Princess Nourah bint Abdulrahman University, P.O. Box 84428, Riyadh, 11671, Saudi Arabia
[f] Department of Mathematics, College of Science, Qassim University, Buraydah, 51452, Saudi Arabia

ARTICLE INFO

Keywords:
Statistical Model
Generalized family of distributions
T-X method
Rényi entropy
Maximum likelihood estimation
Radiation science

ABSTRACT

Radiation data often exhibit complex structures and patterns, posing significant challenges for statistical modeling and analysis. Traditional models may fail to capture the underlying relationships and behaviors of radiation data, leading to inaccurate predictions and risk assessments. This paper introduces the New Beta Prime-Generalized (NBP-G) family of distributions and applies it to develop a new model called the NBP-Weibull distribution. The NBP-Weibull distribution offers enhanced distributional flexibility, capable of representing a wide range of density shapes, including sharply right-skewed and near-symmetric forms. Additionally, the NBP-Weibull model accommodates various types of increasing hazard rate patterns, including those that increase rapidly after an initial flat period, making it crucial for robust reliability and risk assessment applications in radiation engineering. Some desirable statistical properties of the NBP-G family, including moments, the moment-generating function, Rényi and Tsallis entropies, the stress-strength function, and order statistics, are derived. The parameters of the NBP-G family are estimated using the maximum likelihood estimation method. A Monte Carlo simulation study is conducted to evaluate the performance of the MLE method. The NBP-Weibull model is applied to three radiation datasets, and its performance is evaluated using goodness-of-fit criteria. The results show the NBP-G family provides improved fit under selected criteria for modeling complex data patterns. This research highlights the NBP-Weibull model's effectiveness in modeling radiation data and its potential for accurate predictions and insights in this field.

1. Introduction

The analysis of lifetime data is a vital aspect of various fields, including medical science, engineering, and reliability studies, where the accurate modeling of complex phenomena is essential for informed decision-making, risk assessment, and predictive analytics (Elgarhy et al., 2025). Radiation data, in particular, pose significant challenges due to their inherent complexity, variability, and uncertainty, which may arise from various sources, including measurement errors, sampling biases, and underlying physical processes. Recent studies have highlighted the need for novel statistical distributions that can effectively capture the underlying patterns and behaviors of such data, including non-standard shapes, skewness, and heavy tails, which are common characteristics of radiation data (Sun et al., 2026/03; Liu et al., 2026/03; Luo & Luo, 2026/03; Feng et al., 2026). The development of such models is critical for ensuring the accuracy and reliability of predictions, which can have significant consequences in fields such as nuclear engineering, medicine, and environmental science (Althobaiti et al., 2025; Suleiman et al., 2025a, 2025b). As a result, there is a growing demand for innovative statistical approaches that can provide a better understanding of radiation data and improve our ability to analyze and predict complex phenomena (Huang & Ali, 2026; Tung et al., 2026; Zhang et al.,

* Corresponding author.
E-mail addresses: ahmadabubakar31@gmail.com (A.A. Suleiman), Zalthebiti@ut.edu.sa (Z.F. Althobaiti), hanita_daud@utp.edu.my (H. Daud), nazreen@utem.edu.my (N. Waeleh), meabdelwahab@pnu.edu.sa (M.E.A. Elwahab), R.idress@qu.edu.sa (R. Idress).

https://doi.org/10.1016/j.jrras.2026.102432
Received 27 February 2026; Received in revised form 5 April 2026; Accepted 30 April 2026

2026).

Radiation data often arise from complex physical and biological processes, where variability is influenced by factors such as exposure intensity, material heterogeneity, and environmental conditions. These processes frequently produce data with non-standard statistical characteristics, including skewness, heavy tails, and evolving hazard rates. Traditional models are often inadequate in capturing these features simultaneously, leading to inaccurate risk assessment and prediction (Suleiman et al., 2025c). This motivates the development of more flexible statistical models that can better represent the underlying mechanisms of radiation-related phenomena and improve analytical accuracy in practical applications (Ishaq et al., 2023; Yu et al., 2024).

The complexity of radiation data can be attributed to various factors, including the type of radiation, the material being irradiated, and the experimental conditions. These factors can lead to a wide range of data distributions, from simple to complex, and can exhibit various shapes, such as skewness, multimodality, and heavy tails (AlTwijri et al., 2026). Traditional statistical models, such as the Weibull distribution, may not always provide the best fit for such complex data and may lead to inaccurate predictions and conclusions (Basu & Ng, 2025; Gong et al., 2025; Rahmouni & Ziedan, 2025; Tu et al., 2025). Therefore, there is a need for more flexible and robust statistical models that can capture the underlying patterns and behaviors of radiation data. Such models can provide a more accurate understanding of the data, improve predictive analytics, and inform decision-making in various fields (Panitanarak et al., 2025a; Semary et al., 2025a).

In recent years, researchers have proposed various statistical distributions and models to analyze biomedical and radiation data, including generalizations of classical distributions, such as the Weibull distribution, which has enhanced the accuracy of predictions (Ishaq et al., 2025; Panitanarak, Ishaq, et al., 2025; Çolak et al., 2023). For instance, Huo et al. (Huo et al., 2026/03) developed the Log-Lévy distribution and applied it to radiation data. Similarly, Al-Nefaie (Al-Nefaie, 2023/03) introduced the Kavya-Manoharan log-logistic distribution and applied it to biomedical data. Furthermore, Kamal et al. (Kamal et al., 2023) proposed the generalized exponential-Weibull model and explored its application in COVID-19 patient survival times and mortality rate datasets. A comprehensive review of related studies can be found in (Ahmed et al., 2026; Alsaab, 2024; Alsulami & Alghamdi, 2025; Gasper et al., 2025; Gillariose et al., 2025; Hashem et al., 2024; Imran et al., 2024; Khan & Ruidas, 2025; Klakattawi, 2022; Lu et al., 2023; Semary et al., 2025b; Suleiman et al., 2025d; Wu et al., 2023) and the references cited therein. These models have shown promise in capturing the complexity of radiation data, but further research is needed to develop more robust and flexible models that can accommodate the unique characteristics of radiation data.

Classical statistical models, such as the Weibull, exponential, and gamma distributions, are widely used to model biomedical and radiation phenomena due to their foundational properties (Adepoju et al., 2025; Osi et al., 2025). The two-parameter Weibull distribution is particularly common and efficient for analyzing radiation data, but its versatility becomes significantly constrained when dealing with highly complex data exhibiting extreme characteristics. Such data, often characterized by pronounced skewness and heavy or fat tails, deviate significantly from the assumptions of classical distributions (Abd Elgawad et al., 2025). Furthermore, many physical processes, including failure rates in irradiated materials or disease risks, display non-monotonic hazard rates, which the standard two-parameter Weibull model cannot accommodate (Noori et al., 2025). To address these limitations, this study aims to develop a new statistical model, the New Beta Prime Generalized (NBP-G) family of distributions, which can effectively capture the complexity of radiation data. The NBP-G family is based on the Beta Prime (BP) distribution, a univariate model recognized for its efficacy in fitting skewed data across various scientific domains, including engineering and medical science. Specifically, we will utilize the NBP-G family to develop a new distribution called the NBP-Weibull distribution, which offers enhanced distributional flexibility and can represent a wide range of density shapes, including sharply right-skewed and near-symmetric forms. The NBP-Weibull model also accommodates various types of increasing hazard rate patterns, making it suitable for robust reliability and risk assessment applications in radiation engineering. We will apply the NBP-Weibull model to radiation data and evaluate its performance using various metrics, including goodness-of-fit tests and predictive accuracy. The probability density function (PDF) of the BP distribution with shape parameters is provided as follows:

The probability density function (PDF) of the BP distribution with shape parameters $\alpha, \beta > 0$ is provided as follows:

$$m(x;\alpha,\beta) = \frac{x^{\alpha-1}}{B(\alpha,\beta)(1+x)^{\alpha+\beta}}, x > 0; \quad \alpha,\beta > 0, \tag{1}$$

where $B(\alpha,\beta) = \int_0^\infty \frac{\omega^{\alpha-1}}{(1+\omega)^{\alpha+\beta}} d\omega$ represents the BP (Beta of the Second Kind) function. The corresponding cumulative distribution function (CDF) is presented as follows:

$$M(x;\alpha,\beta) = \frac{B_x(\alpha,\beta)}{B(\alpha,\beta)}, x > 0; \quad \alpha,\beta > 0, \tag{2}$$

where $B_x(\alpha,\beta) = \int_0^x \frac{\omega^{\alpha-1}}{(1+\omega)^{\alpha+\beta}} d\omega$ is the incomplete BP function.

Alzaatreh et al. (Alzaatreh et al., 2013) presented the T-X method, a comprehensive approach to generate new classes of continuous probability distributions that can handle any range of probability measures. This method incorporates an auxiliary random variable V, defined on a bounded interval, into the target distribution. Let X be a random variable with PDF $g(x)$ and CDF $G(x)$. Let V be another continuous random variable with PDF $h(v)$ and CDF $H(v)$, defined over $[a,b]$. Using the T-X method, the new CDF $F(x)$ is expressed as:

$$F(x) = \int_a^{T(G(x))} h(v)dv = H(T(G(x))), \tag{3}$$

where $T(G(x))$ is a transformation function applied to the baseline CDF $G(x)$. The T-X approach has been widely employed to develop generalized probability distributions that can capture complex features such as skewness, kurtosis, and heavy tails, making them useful in various applications, including radiation data analysis (see (Alzaatreh et al., 2013) for more details). In this study, we utilize the T-X approach, which integrates an auxiliary random variable with the target distribution via a transformation function, to develop a new generalized probability distribution. This approach is recognized for its effectiveness in capturing complex features such as skewness, kurtosis, and heavy tails, making it highly useful for modeling radiation data and other applications.

Despite the extensive development of generalized distributions using transformation techniques such as the T-X method, many existing models remain limited in their ability to simultaneously capture complex skewness, tail behavior, and diverse hazard rate structures observed in real-world data, particularly in radiation studies. Most existing generalizations, including Beta-G (Eugene et al., 2002) and Kumaraswamy-G (Cordeiro & De Castro, 2011) families, rely on bounded transformations that may restrict flexibility in modeling heavy-tailed phenomena.

The proposed NBP-G family addresses this limitation by incorporating the Beta Prime structure within the T-X framework, introducing an additional exponent parameter that enhances adaptability. This results in improved capability to model both extreme skewness and varying hazard rate behaviors. Furthermore, the NBP-Weibull model provides a flexible five-parameter structure that can accommodate a

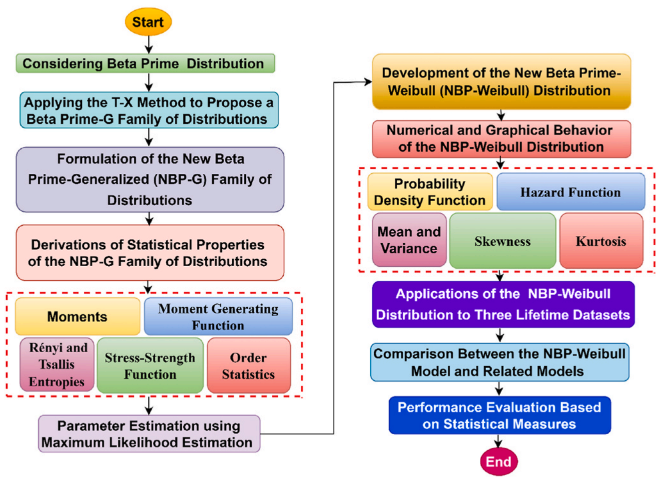

Fig. 1. Flowchart for the development of the BP-G family and the NBP-Weibull model.

wide range of distributional shapes and reliability patterns. In contrast to existing models, the proposed approach offers a unified framework that combines theoretical tractability with practical applicability, particularly for modeling radiation data characterized by high variability and complex failure mechanisms.

The motivation for developing a highly flexible model such as the NBP-Weibull distribution is critically tied to its application in analyzing complex reliability and exposure data, particularly in the context of radiation datasets. This study focuses on radiation datasets concerning the susceptibility index (SI) of organic materials, specifically peppermint packets, following exposure to gamma or microwave irradiation. The Susceptibility Index (SI) measures a material's resistance to biological infestation after treatment, with factors such as dose uniformity, material heterogeneity, and complex biological responses introducing substantial variability into the observed data. This variability often results in distributions that exhibit extreme skewness, high kurtosis, and complex reliability trends. These complex structures cannot be adequately captured by the traditional Weibull models. Given these limitations, the NBP-Weibull distribution, with its five parameters, offers a statistically improved fit. This enables more reliable risk assessment and treatment efficacy evaluation in radiation science. Fig. 1 illustrates the flow for the proposed NBP-G family and NBP-Weibull sub-model, visually representing the steps involved in deriving, analyzing, and estimating the parameters of the NBP-G family and NBP-Weibull model.

This paper introduces the NBP-Weibull distribution, making the following significant theoretical and practical contributions to advanced radiation research.

i. To develop the NBP-G family of distributions based on the T-X method, providing a versatile framework for extending any continuous baseline model.
ii. To pioneer the five-parameter NBP-Weibull model, addressing the limitations of traditional generalized Weibull models by significantly enhancing flexibility in modeling complex data patterns, particularly those found in radiation susceptibility studies.
iii. To offer a higher degree of flexibility, capable of representing a wide range of density shapes, including sharply right-skewed, left-skewed, and near-symmetric forms.
iv. To accommodate various types of increasing hazard rate patterns, including those that increase rapidly after an initial flat period, which is crucial for robust reliability and risk assessment applications in radiation engineering.
v. To introduce extensive mathematical properties, including mixture representations, moments, moment-generating function (MGF), Rényi and Tsallis entropies, stress-strength function, and order statistics.
vi. To analyze parameter estimation using Maximum Likelihood Estimation (MLE).
vii. To conduct a Monte Carlo simulation study to demonstrate the performance of the parameters and evaluate the finite-sample behavior of the MLEs.
viii. To demonstrate the model's effectiveness through its improved fit to three distinct real-world radiation susceptibility datasets, outperforming several established competing models based on statistical criteria.

The remaining sections of this paper are structured as follows: Section 2 details the construction and derivation of the NBP-G family. Section 3 introduces the NBP-Weibull model and analyzes its distribution shapes. Section 4 presents the statistical properties of the NBP-G family. Section 5 discusses parameter estimation via MLE. Section 6 performs the Monte Carlo simulation study. Section 7 provides the application and analysis using three radiation datasets. Section 8 concludes the study, discussing limitations and future research directions.

2. Formulation of the New Beta Prime-Generalized (NBP-G) family of distributions

This section introduces the NBP-G family, which employs the T-X approach developed by Alzaatreh et al. (Alzaatreh et al., 2013). The proposed methodology involves deriving the CDF of the NBP-G family by substituting baseline components into (3). The link function $T(G(x)) = \left(\frac{G(x;\eta)}{1-G(x;\eta)}\right)^{\lambda}$ and PDF of the BP distribution from (1) are specifically utilized to construct the new NBP-G family of distributions as follows:

$$F(x;\alpha,\beta,\lambda,\eta) = \frac{1}{B(\alpha,\beta)} \int_0^{\left(\frac{G(x;\eta)}{1-G(x;\eta)}\right)^{\lambda}} \frac{t^{\alpha-1}}{(1+t)^{\alpha+\beta}} dt. \tag{4}$$

Let:

$$t = \frac{m}{1-m}, \Rightarrow \quad m = \frac{t}{1+t}, \text{and} \quad dt = \frac{dm}{(1-m)^2}. \tag{5}$$

Substituting (5) into (4) gives the following expression:

$$F(x;\alpha,\beta,\lambda,\eta) = \frac{1}{B(\alpha,\beta)} \int_0^{\frac{\left(\frac{G(x;\eta)}{1-G(x;\eta)}\right)^{\lambda}}{1+\left(\frac{G(x;\eta)}{1-G(x;\eta)}\right)^{\lambda}}} \frac{\left(\frac{m}{1-m}\right)^{\alpha-1}}{\left(1+\left(\frac{m}{1-m}\right)\right)^{\alpha+\beta}} \frac{dm}{(1-m)^2}$$

$$= \frac{1}{B(\alpha,\beta)} \int_0^{\frac{\left(\frac{G(x;\eta)}{1-G(x;\eta)}\right)^{\lambda}}{1+\left(\frac{G(x;\eta)}{1-G(x;\eta)}\right)^{\lambda}}} \frac{m^{\alpha-1}}{(1-m)^{\alpha-1+2}\left(\frac{1-m+m}{1-m}\right)^{\alpha+\beta}} dm$$

$$= \frac{1}{B(\alpha,\beta)} \int_0^{\frac{\left(\frac{G(x;\eta)}{1-G(x;\eta)}\right)^{\lambda}}{1+\left(\frac{G(x;\eta)}{1-G(x;\eta)}\right)^{\lambda}}} \frac{m^{\alpha-1}}{(1-m)^{\alpha+1}(1-m)^{-\alpha-\beta}} dm$$

$$= \frac{1}{B(\alpha,\beta)} \int_0^{\frac{\left(\frac{G(x;\eta)}{1-G(x;\eta)}\right)^{\lambda}}{1+\left(\frac{G(x;\eta)}{1-G(x;\eta)}\right)^{\lambda}}} m^{\alpha-1}(1-m)^{\beta-1} dm$$

$$= \frac{1}{B(\alpha,\beta)} B_{w(x;\lambda,\eta)}(\alpha,\beta), x \in \mathbb{R}; \quad \alpha,\beta,\lambda > 0, \tag{6}$$

where $B_{w(x;\lambda,\eta)}(\alpha,\beta) = \int_0^{w(x;\lambda,\eta)} m^{\alpha-1}(1-m)^{\beta-1}dm$, $w(x;\lambda,\eta) = \frac{\left(\frac{G(x;\eta)}{1-G(x;\eta)}\right)^{\lambda}}{1+\left(\frac{G(x;\eta)}{1-G(x;\eta)}\right)^{\lambda}}$ and $G(x;\eta)$ is the CDF of the parent distribution with the vector parameter η, while α and β represents the shape parameters, and λ is an exponent parameter. It can be observed from (6) that the CDF of the NBP-G family reduces to the Beta-G family of distributions, as proposed by Eugene et al. (Eugene et al., 2002), when $\lambda = 1$.

Differentiating (6) with respect to x provides the PDF for the NBP-G family of distributions as follows:

$$f(x;\alpha,\beta,\lambda,\eta) = \frac{d}{dx}[F(x;\alpha,\beta,\lambda,\eta)]$$

$$= \frac{1}{B(\alpha,\beta)} \quad \frac{d}{dx}\left(B_{w(x;\lambda,\eta)}(\alpha,\beta)\right),$$

$$= \frac{1}{B(\alpha,\beta)}(w(x;\lambda,\eta))^{\alpha-1}(1-w(x;\lambda,\eta))^{\beta-1} \times \frac{d}{dx}(w(x;\lambda,\eta)).$$

$$= \frac{1}{B(\alpha,\beta)}(w(x;\lambda,\eta))^{\alpha-1}(1-w(x;\lambda,\eta))^{\beta-1} \times \frac{\lambda g(x;\eta)\left(\frac{G(x;\eta)}{1-G(x;\eta)}\right)^{\lambda-1}}{(1-G(x;\eta))^2\left\{1+\left(\frac{G(x;\eta)}{1-G(x;\eta)}\right)^{\lambda}\right\}^2}$$

$$= \frac{\lambda g(x;\eta)\left(\frac{G(x;\eta)}{1-G(x;\eta)}\right)^{\lambda-1}}{B(\alpha,\beta)(1-G(x;\eta))^2} \frac{w^{\alpha-1}(x;\lambda,\eta)(1-w(x;\lambda,\eta))^{\beta-1}}{\left\{1+\left(\frac{G(x;\eta)}{1-G(x;\eta)}\right)^{\lambda}\right\}^2}$$

$$= \frac{\lambda g(x;\eta)G^{\lambda-1}(x;\eta)}{B(\alpha,\beta)(1-G(x;\eta))^{\lambda+1}} \frac{w^{\alpha-1}(x;\lambda,\eta)(1-w(x;\lambda,\eta))^{\beta-1}}{\left\{1+\left(\frac{G(x;\eta)}{1-G(x;\eta)}\right)^{\lambda}\right\}^2}, x \in \mathbb{R}, \alpha,\beta,\lambda > 0, \tag{7}$$

where α and β are the shape parameters, λ is an exponent parameter, $g(x;\eta)$ and $G(x;\eta)$ are the PDF and CDF of the parent distribution with vector parameter η. Hence, (7) represents the PDF of the proposed NBP-G family of distributions, where $g(x;\eta)$ is the PDF of the parent distribution. The random variable X defined with PDF in (7) can now be expressed as $X \sim NBP - G(\alpha,\beta,\lambda,\eta)$. This denotes the NBP-G family with parameters α, β, λ, and η. For simplicity, the dependence on α, β, λ, and η can be omitted by denoting the CDF and PDF as $F(x;\alpha,\beta,\lambda,\eta) = F(x)$ and $f(x;\alpha,\beta,\lambda,\eta) = f(x)$, respectively.

2.1. Expansion for the CDF and PDF of the NBP-G family of distributions

In this subsection, the focus is on deriving structured representations of the CDF and PDF for the NBP-G family. These structured forms aim to enhance both theoretical understanding and computational efficiency. Specifically, the CDF and PDF are expressed in linear and series forms that retain the generality of the NBP-G family while simplifying complex expressions. The linear representation refers to expressing the functions in a compact, interpretable format using basic algebraic components. The CDF of the NBP-G family is expanded as:

$$F(x) = \frac{B_{\Delta}(\alpha,\beta)}{B(\alpha,\beta)} = \mathrm{I}_{\Delta}(\alpha,\beta), \Delta = w(x;\lambda,\eta) = \frac{\left(\frac{G(x;\eta)}{1-G(x;\eta)}\right)^{\lambda}}{1+\left(\frac{G(x;\eta)}{1-G(x;\eta)}\right)^{\lambda}}. \tag{8}$$

Cordeiro and Nadarajah (Cordeiro & Nadarajah, 2011) and Biazatti et al. (Biazatti et al., 2022) provide a structured expansion for the CDF described in (8) as:

$$\mathrm{I}_{\Delta}(\alpha,\beta) = \frac{\Delta^{\alpha}}{B(\alpha,\beta)} \sum_{i=0}^{\infty} \pi_i \Delta^i. \tag{9}$$

where $\pi_i = \frac{(1-\beta)_i}{(\alpha+i)i!}$ and $(w)_i = w(w-1)\cdots(w-i+1)$ is defined as falling factorial, for $w = 1-\beta$.

Therefore, (9) can be expressed as:

$$\mathrm{I}_{\Delta}(\alpha,\beta) = \frac{1}{B(\alpha,\beta)} \sum_{i=0}^{\infty} \pi_i \frac{\left\{\left(\frac{G(x;\eta)}{1-G(x;\eta)}\right)^{\lambda}\right\}^{i+\alpha}}{\left\{1+\left(\frac{G(x;\eta)}{1-G(x;\eta)}\right)^{\lambda}\right\}^{i+\alpha}}. \tag{10}$$

The generalized binomial expansions for any real number ϑ with $|z| < 1$, as discussed in Kreyszig (Kreyszig, 2007), can be expressed as:

$$(1+z)^{-\vartheta} = \sum_{j=0}^{\infty} (-1)^j \binom{\vartheta+j-1}{j} z^j, \tag{11}$$

and

$$(1-z)^{-\vartheta} = \sum_{p=0}^{\infty} \binom{\vartheta+p-1}{p} z^p. \tag{12}$$

Applying (11) to the denominator of (10) results in:

$$\mathrm{I}_{\Delta}(\alpha,\beta) = \frac{1}{B(\alpha,\beta)} \sum_{i,j=0}^{\infty} \pi_i (-1)^j \binom{i+\alpha+j-1}{j} \frac{G^{\lambda(i+\alpha+j)}(x;\eta)}{(1-G(x;\eta))^{\lambda(i+\alpha+j)}}. \tag{13}$$

Considering (12), then (13) yields the CDF of the NBP-G family of distributions as:

$$\mathrm{I}_{\Delta}(\alpha,\beta) = \sum_{i,j,p=0}^{\infty} A_{i,j,p}\{G(x;\eta)\}^{\lambda(i+\alpha+j)+p} \tag{14}$$

where $A_{i,j,p} = \frac{\pi_i(-1)^j}{B(\alpha,\beta)} \binom{i+\alpha+j-1}{j} \binom{\lambda(i+\alpha+j)+p-1}{p}$.

The PDF of the NBP-G family of distributions is obtained by applying the binomial expansion, where ϑ is a non-negative number and $\vartheta > 0$ with $|z| < 1$, as outlined in Arfken and Weber (Arfken et al., 2005) and Stewart et al. (Stewart et al., 2021). It can be expressed as follows:

$$(1-z)^{\vartheta} = \sum_{k=0}^{\infty} (-1)^k \binom{\vartheta}{k} z^k. \tag{15}$$

The series and binomial expansions used in this study are valid under standard convergence conditions, particularly when the transformed variable satisfies $|z| < 1$. The exponential decay properties of the underlying functions ensure rapid convergence, and in practical computations, only a finite number of terms are required to achieve accurate approximations.

Applying (15) to the last term of (7) becomes:

$$f(x)=\frac{\lambda g(x;\eta)}{B(\alpha,\beta)}\sum_{k=0}^{\infty}\left\{\frac{(-1)^{k}\binom{\beta-1}{k}G^{\lambda+\lambda(\alpha+k-1)-1}(x;\eta)}{(1-G(x;\eta))^{\lambda+\lambda(\alpha+k-1)+1}\left\{1+\left(\frac{G(x;\eta)}{1-G(x;\eta)}\right)^{\lambda}\right\}^{2+\alpha+k-1}}\right\}$$

$$=\frac{\lambda g(x;\eta)}{B(\alpha,\beta)}\sum_{k,j=0}^{\infty}\frac{(-1)^{k+j}\binom{\beta-1}{k}\binom{\alpha+k+j}{j}G^{\lambda+\lambda(\alpha+k-1)+\lambda j-1}(x;\eta)}{(1-G(x;\eta))^{\lambda+\lambda(\alpha+k-1)+\lambda j+1}}$$

$$=g(x;\eta)\sum_{k,j,p=0}^{\infty}C_{k,j,p}G^{\lambda(\alpha+k)+\lambda j+p-1}(x;\eta), \tag{16}$$

where $C_{k,j,p}=\frac{\lambda(-1)^{k+j}\binom{\beta-1}{k}\binom{\alpha+k+j}{j}\binom{\lambda(\alpha+k)+\lambda j+p}{p}}{B(\alpha,\beta)}$, α and β are the shape parameters, λ is an exponent parameter, $g(x;\eta)$ and $G(x;\eta)$ are the PDF and CDF of the parent distribution with a vector parameter η.

2.2. Validity Check of the NBP-G family of distributions

To verify the validity of the proposed NBP-G family as a legitimate probability distribution, its PDF, as defined in (7), must satisfy the condition:

$$\int_{-\infty}^{\infty}f(x)dx=1. \tag{17}$$

Substituting (7) into (17), we have:

$$\int_{-\infty}^{\infty}f(x)dx=\frac{\lambda}{B(\alpha,\beta)}\int_{-\infty}^{\infty}\frac{g(x;\eta)G^{\lambda-1}(x;\eta)}{(1-G(x;\eta))^{\lambda+1}}\frac{\left\{\frac{\left(\frac{G(x;\eta)}{1-G(x;\eta)}\right)^{\lambda}}{1+\left(\frac{G(x;\eta)}{1-G(x;\eta)}\right)^{\lambda}}\right\}^{\alpha-1}\left(1-\left(\frac{\left(\frac{G(x;\eta)}{1-G(x;\eta)}\right)^{\lambda}}{1+\left(\frac{G(x;\eta)}{1-G(x;\eta)}\right)^{\lambda}}\right)\right)^{\beta-1}}{\left\{1+\left(\frac{G(x;\eta)}{1-G(x;\eta)}\right)^{\lambda}\right\}^{2}}dx.. \tag{18}$$

Let:

$$y=\frac{\left(\frac{G(x;\eta)}{1-G(x;\eta)}\right)^{\lambda}}{1+\left(\frac{G(x;\eta)}{1-G(x;\eta)}\right)^{\lambda}},\text{ this implies, }dx=\frac{(1-G(x;\eta))^{2}\left\{1+\left(\frac{G(x;\eta)}{1-G(x;\eta)}\right)^{\lambda}\right\}^{2}}{\lambda g(x;\eta)\left(\frac{G(x;\eta)}{1-G(x;\eta)}\right)^{\lambda-1}}dy. \tag{19}$$

Substituting (19) into (18) results in the following expression:

$$\int_{-\infty}^{\infty}f(x)dx=\frac{1}{B(\alpha,\beta)}\int_{0}^{1}\frac{G^{\lambda-1}(x;\eta)}{(1-G(x;\eta))^{\lambda+1}}\frac{(1-G(x;\eta))^{2}}{\left(\frac{G(x;\eta)}{1-G(x;\eta)}\right)^{\lambda-1}}y^{\alpha-1}(1-y)^{\beta-1}dy$$

$$=\frac{1}{B(\alpha,\beta)}\int_{0}^{1}y^{\alpha-1}(1-y)^{\beta-1}dy$$

$$=1. \tag{20}$$

Thus, the condition $\int_{-\infty}^{\infty}f(x)dx=1$ is satisfied, confirming that the NBP-G family's PDF is a valid statistical probability distribution.

The survival and hazard functions of the NBP-G family of distributions are presented as follows:

$$S(x)=1-\frac{B_{w(x;\lambda,\eta)}(\alpha,\beta)}{B(\alpha,\beta)};\quad x\in\mathbb{R},\alpha,\beta>0, \tag{21}$$

and

$$h(x)=\frac{\lambda g(x;\eta)G^{\lambda-1}(x;\eta)w^{\alpha-1}(x;\lambda,\eta)(1-w(x;\lambda,\eta))^{\beta-1}}{(1-G(x;\eta))^{\lambda+1}\left\{1+\left(\frac{G(x;\eta)}{1-G(x;\eta)}\right)^{\lambda}\right\}^{2}\left\{B(\alpha,\beta)-B_{w(x;\lambda,\eta)}(\alpha,\beta)\right\}};$$

$$x\in\mathbb{R},\alpha,\beta>0, \tag{22}$$

respectively, where $w(x;\lambda,\eta)=\frac{\left(\frac{G(x;\eta)}{1-G(x;\eta)}\right)^{\lambda}}{1+\left(\frac{G(x;\eta)}{1-G(x;\eta)}\right)^{\lambda}}$.

2.3. Quantile function

The quantile function of a probability distribution is a crucial tool for understanding the distribution of random variable occurrences. It is widely employed in simulation studies to generate random numbers, compute the median, and derive other key statistics. For the proposed NBP-G family, the quantile function can be obtained by inverting the CDF defined in (6), this process yields the quantile function as:

$$\frac{\left(\frac{G(x;\eta)}{1-G(x;\eta)}\right)^{\lambda}}{1+\left(\frac{G(x;\eta)}{1-G(x;\eta)}\right)^{\lambda}}=I^{-1}(u,\alpha,\beta), \tag{23}$$

where u is a uniform random variable on the interval (0,1) and $I^{-1}(u,\alpha,\beta)$ denotes the inverse of the regularized incomplete Beta function, i.e., the value of Δ such that $I_{\Delta}(\alpha,\beta)=u$ is the $u-th$ quantile of the $B(\alpha,\beta)$ distribution. To obtain the quantile function of the parent model, therefore (23) can be reformulated as:

$$G(x;\eta)=\frac{E^{\frac{1}{\lambda}}}{1+E^{\frac{1}{\lambda}}},E=\frac{I^{-1}(u,\alpha,\beta)}{1-I^{-1}(u,\alpha,\beta)}. \tag{24}$$

This implies,

$$G(x;\eta)=\frac{E^{\frac{1}{\lambda}}}{1+E^{\frac{1}{\lambda}}}. \tag{25}$$

Therefore, the inverse transformation approach in (25) gives the quantile function of the NBP-G family expressed as:

$$x_q(u) = G^{-1}\left\{\frac{E^{\frac{1}{\lambda}}}{1+E^{\frac{1}{\lambda}}}\right\}. \tag{26}$$

The median of the proposed NBP-G family can be calculated by setting $u = 0.5$ in the quantile function, resulting in:

$$x_q(0.5) = G^{-1}\left\{\frac{\left\{\frac{I^{-1}(0.5,\alpha,\beta)}{1-I^{-1}(0.5,\alpha,\beta)}\right\}^{\frac{1}{\lambda}}}{1+\left\{\frac{I^{-1}(0.5,\alpha,\beta)}{1-I^{-1}(0.5,\alpha,\beta)}\right\}^{\frac{1}{\lambda}}}\right\}. \tag{27}$$

The proposed NBP-G family differs from existing generalized families, such as the Beta-G (Eugene et al., 2002), Kumaraswamy-G (Cordeiro & De Castro, 2011), Gamma-G (Jones, 2004), and Beta Prime-G (Suleiman et al., 2023) distributions in several key aspects. While the Beta-G and Kumaraswamy-G families rely on bounded transformations, the NBP-G family is constructed using the Beta Prime structure, which allows for greater flexibility in modeling heavy-tailed and skewed data. Unlike the standard Beta Prime-G family, the inclusion of an additional exponent parameter enhances the model's adaptability to capture diverse shapes of the PDF and hazard function. Furthermore, the NBP-G family provides improved control over tail behavior and hazard rate dynamics, making it particularly suitable for complex datasets such as radiation data.

3. Statistical properties of the NBP-G family of distributions

This section introduces the key statistical properties of the NBP-G family of distributions, including the derivation of moments, the moment generating function (MGF), Rényi and Tsallis entropies, the stress-strength function, and order statistics. These properties are essential for comprehensive modeling and analysis, providing insights into the distribution's behavior and applications in various fields.

3.1. Moments

The moments of the NBP-G family are determined using the PDF defined in (16) as:

$$E(X^r) = \sum_{k,j,p=0}^{\infty} C_{k,j,p} \int_{-\infty}^{\infty} x^r g(x;\eta) G^{\lambda(\alpha+k)+\lambda j+p-1}(x;\eta)dx, \tag{28}$$

where r is a positive integer and $C_{k,j,p} = \frac{\lambda(-1)^{k+j}\binom{\beta-1}{k}\binom{\alpha+k+j}{j}\binom{\lambda(\alpha+k)+\lambda j+p}{p}}{B(\alpha,\beta)}$. This simplifies as:

$$E(X^r) = \sum_{k,j,p=0}^{\infty} C_{k,j,p} \int_{-\infty}^{\infty} x^r z_{k,j,p}(x;\eta)dx, \tag{29}$$

where $z_{k,j,p}(x;\eta) = g(x;\eta)G^{\lambda(\alpha+k)+\lambda j+p-1}(x;\eta)$, $G(x;\eta)$ and $g(x;\eta)$ are the CDF and PDF of the parent distributions, respectively. These moments provide essential measures for characterizing the NBP-G family.

3.2. Moment generating function

The moment generating function (MGF) of the NBP-G family of distributions can be derived using the PDF of the NBP-G family described in Equation (16):

$$M_X(t) = \sum_{k,j,p=0}^{\infty} C_{k,j,p} \int_{-\infty}^{\infty} e^{tx} g(x;\eta) G^{\lambda(\alpha+k)+\lambda j+p-1}(x;\eta)dx. \tag{30}$$

Expanding the exponential term e^{tx} using its series expansion:

$$e^{tx} = \sum_{r=0}^{\infty}\frac{(tx)^r}{r!}, \tag{31}$$

and substituting this expansion into (33) yields:

$$M_X(t) = \sum_{k,j,p,r=0}^{\infty} C_{k,j,p}\frac{t^r}{r!}\int_{-\infty}^{\infty} x^r g(x;\eta)G^{\lambda(\alpha+k)+\lambda j+p-1}(x;\eta)dx$$

$$= \sum_{r=0}^{\infty}\frac{t^r}{r!}\left\{\sum_{k,j,p=0}^{\infty} C_{k,j,p}\int_{-\infty}^{\infty} x^r z_{k,j,p}dx\right\}$$

$$= \sum_{r=0}^{\infty}\frac{t^r}{r!}E(X^r), \tag{32}$$

where $E(X^r)$ corresponds to the r^{th} moments of the NBP-G family of distributions as defined in (29).

3.3. Entropies

The Rényi and Tsallis entropies are significant measures in quantifying the uncertainty or disorder within a probability distribution. These entropy measures for the NBP-G family of distributions are derived using the PDF defined in (7).

3.3.1. Rényi entropy

The Rényi entropy of the random variable X with PDF in (7) is defined as:

$$R_\tau(X) = \frac{1}{1-\tau}\log\left[\int_{-\infty}^{\infty} f^\tau(x)dx\right], x\in\mathbb{R}, 0<\tau<\infty, \tau\neq 1, \tag{33}$$

For computing the Rényi entropy of the NBP-G family, the integrand in (33) is formulated as:

$$f^\tau(x) = \frac{\lambda^\tau g^\tau(x;\eta)G^{\tau(\lambda-1)}(x;\eta)}{\{B(\alpha,\beta)\}^\tau(1-G(x;\eta))^{\tau(\lambda+1)}}\,\frac{w^{\tau(\alpha-1)}(x;\lambda,\eta)(1-w(x;\lambda,\eta))^{\tau(\beta-1)}}{\left\{1+\left(\frac{G(x;\eta)}{1-G(x;\eta)}\right)^\lambda\right\}^{2\tau}}. \tag{34}$$

Using the expansion defined in (15), the integrand simplifies to:

$$f^\tau(x) = \frac{\lambda^\tau g^\tau(x;\eta)G^{\tau(\lambda-1)}(x;\eta)}{\{B(\alpha,\beta)\}^\tau(1-G(x;\eta))^{\tau(\lambda+1)}\left\{1+\left(\frac{G(x;\eta)}{1-G(x;\eta)}\right)^\lambda\right\}^{2\tau}} \sum_{k=0}^{\infty}\left\{(-1)^k\binom{\tau(\beta-1)}{k}w^{\tau(\alpha-1)+k}(x;\lambda,\eta)\right\}$$

$$= \frac{\lambda^\tau g^\tau(x;\eta)G^{\tau(\lambda-1)}(x;\eta)}{\{B(\alpha,\beta)\}^\tau(1-G(x;\eta))^{\tau(\lambda+1)}\left\{1+\left(\frac{G(x;\eta)}{1-G(x;\eta)}\right)^\lambda\right\}^{2\tau}} \left\{\sum_{k=0}^{\infty}(-1)^k\binom{\tau(\beta-1)}{k}\left\{\frac{\left(\frac{G(x;\eta)}{1-G(x;\eta)}\right)^\lambda}{1+\left(\frac{G(x;\eta)}{1-G(x;\eta)}\right)^\lambda}\right\}^{\tau(\alpha-1)+k}\right\}$$

$$= \frac{\lambda^{\tau} g^{\tau}(x;\eta) G^{\tau(\lambda-1)}(x;\eta)}{\{B(\alpha,\beta)\}^{\tau}(1-G(x;\eta))^{\tau(\lambda+1)}\left\{1+\left(\frac{G(x;\eta)}{1-G(x;\eta)}\right)^{\lambda}\right\}^{2\tau}} \left\{\sum_{k=0}^{\infty}(-1)^k \binom{\tau(\beta-1)}{k} \frac{\left\{\left(\frac{G(x;\eta)}{1-G(x;\eta)}\right)^{\lambda}\right\}^{\tau(\alpha-1)+k}}{\left\{1+\left(\frac{G(x;\eta)}{1-G(x;\eta)}\right)^{\lambda}\right\}^{\tau(\alpha-1)+k}}\right\}$$

$$= \frac{\lambda^{\tau} g^{\tau}(x;\eta) G^{\tau(\lambda-1)}(x;\eta)}{\{B(\alpha,\beta)\}^{\tau}(1-G(x;\eta))^{\tau(\lambda+1)}} \left\{\sum_{k=0}^{\infty}(-1)^k \binom{\tau(\beta-1)}{k} \frac{\left\{\left(\frac{G(x;\eta)}{1-G(x;\eta)}\right)^{\lambda}\right\}^{\tau(\alpha-1)+k}}{\left\{1+\left(\frac{G(x;\eta)}{1-G(x;\eta)}\right)^{\lambda}\right\}^{\tau(\alpha-1)+k+2\tau}}\right\}. \tag{35}$$

Based on (11), then we can rewrite (35) as:

$$f^{\tau}(x) = \frac{\lambda^{\tau} g^{\tau}(x;\eta)}{\{B(\alpha,\beta)\}^{\tau}} \sum_{k,j=0}^{\infty}(-1)^{k+j}\binom{\tau(\beta-1)}{k}\binom{\tau(\alpha-1)+k+2\tau+j-1}{j} \frac{G^{\tau(\lambda-1)+\lambda(\tau(\alpha-1)+k+j)}(x;\eta)}{(1-G(x;\eta))^{\tau(\lambda+1)+\lambda(\tau(\alpha-1)+k+j)}}$$

$$= \sum_{k,j,p=0}^{\infty} \phi_{k,j,p} D_{k,j,p}(x;\eta), \tag{36}$$

where $\phi_{k,j,p} = \frac{\lambda^{\tau}(-1)^{k+j}}{\{B(\alpha,\beta)\}^{\tau}}\binom{\tau(\beta-1)}{k}\binom{\tau(\alpha-1)+k+2\tau+j-1}{j}\binom{\tau(\lambda+1)+\lambda(\tau(\alpha-1)+k+j)+p-1}{p}$ and $D_{k,j,p}(x;\eta) = g^{\tau}(x;\eta)G^{\tau(\lambda-1)+\lambda(\tau(\alpha-1)+k+j)+p}(x;\eta)$.

Substituting (36) into (33) yields the Rényi entropy for the NBP-G family:

$$R_{\tau}(X) = \frac{1}{1-\tau}\log\left[\sum_{k,j,p=0}^{\infty}\phi_{k,j,p}\int_{-\infty}^{\infty} D_{k,j,p}(x;\eta)dx\right]; \quad 0<\tau<\infty, \tau\neq 1. \tag{37}$$

3.3.2. Tsallis entropy

Tsallis entropy for the NBP-G family of distributions is derived based on (37) as follows:

$$T_{\tau}(X) = \frac{\vartheta}{\tau-1}\left[1-\sum_{k,j,p=0}^{\infty}\phi_{k,j,p}\int_{-\infty}^{\infty} D_{k,j,p}(x;\eta)dx\right]. \tag{38}$$

3.4. Stress-strength

The stress-strength model evaluates the probability that a system's strength exceeds the applied stress under given conditions. In this work, the stress (X_1) and strength (X_2) are considered two random variables from the NBP-G family, each with distinct shape parameters, α_1 and α_2, respectively. A key assumption is that both variables share a common shape parameter β, an exponent parameter λ, and along with a parent distribution parameter η. By adopting this assumption of shared parameters, the model's complexity is reduced, enabling a more focused analysis of the role of the individual shape parameters, α_1 and α_2, in determining system reliability. Under these conditions, the stress-strength model of the BP-G family of distributions is defined as:

$$R = \int_{-\infty}^{\infty} f(x_2;\alpha_2,\beta,\lambda,\eta)dx_2 \int_{-\infty}^{x_2} f(x_1;\alpha_1,\beta,\lambda,\eta)dx_1$$

$$= \int_{-\infty}^{\infty} f(x_2;\alpha_2,\beta,\lambda,\eta)F(x_2;\alpha_1,\beta,\lambda,\eta)dx_2, \tag{39}$$

where $F(x_2;\alpha_1,\beta,\lambda,\eta)$ and $f(x_2;\alpha_2,\beta,\lambda,\eta)$ are the CDF and PDF of the NBP-G family. Using (7) and (10), the integrand of (39) gives:

$$f(x_2;\alpha_2,\beta,\lambda,\eta)F(x_2;\alpha_1,\beta,\lambda,\eta) = \frac{\lambda g(x_2;\eta)G^{\lambda-1}(x_2;\eta)}{B(\alpha_2,\beta)B(\alpha_1,\beta)(1-G(x_2;\eta))^{\lambda+1}} \sum_{i=0}^{\infty}\pi_i \frac{\left\{\frac{\left(\frac{G(x_2;\eta)}{1-G(x_2;\eta)}\right)^{\lambda}}{1+\left(\frac{G(x_2;\eta)}{1-G(x_2;\eta)}\right)^{\lambda}}\right\}^{\alpha_2+\alpha_1+i-1}}{\left\{1+\left(\frac{G(x_2;\eta)}{1-G(x_2;\eta)}\right)^{\lambda}\right\}^{2}} \times\left(1-\left\{\frac{\left(\frac{G(x_2;\eta)}{1-G(x_2;\eta)}\right)^{\lambda}}{1+\left(\frac{G(x_2;\eta)}{1-G(x_2;\eta)}\right)^{\lambda}}\right\}\right)^{\beta-1}. \tag{40}$$

Using the generalized binomial expansion in (15), then (40) simplifies to:

$$f(x_2;\alpha_2,\beta,\lambda,\eta)F(x_2;\alpha_1,\beta,\lambda,\eta) = \frac{\lambda g(x_2;\eta)G^{\lambda-1}(x_2;\eta)}{B(\alpha_2,\beta)B(\alpha_1,\beta)(1-G(x_2;\eta))^{\lambda+1}} \sum_{i,k=0}^{\infty}(-1)^k\binom{\beta-1}{k}\pi_i \frac{\left(\frac{G(x_2;\eta)}{1-G(x_2;\eta)}\right)^{\lambda(\alpha_1+\alpha_2+i+k-1)}}{\left\{1+\left(\frac{G(x_2;\eta)}{1-G(x_2;\eta)}\right)^{\lambda}\right\}^{1+\alpha_1+\alpha_2+i+k}}, \tag{41}$$

where $M_{i,k} = \frac{\lambda(-1)^k\pi_i\binom{\beta-1}{k}}{B(\alpha_2,\beta)B(\alpha_1,\beta)}$ and $\nu = \alpha_1+\alpha_2+i+k$.

Considering (11), the integrand of (41) yields:

$$f(x_2;\alpha_2,\beta,\lambda,\eta)F(x_2;\alpha_1,\beta,\lambda,\eta) = \frac{\lambda g(x_2;\eta)}{B(\alpha_2,\beta)B(\alpha_1,\beta)}\sum_{i,k,j=0}^{\infty}(-1)^{k+j}\binom{\beta-1}{k}\binom{\alpha_1+\alpha_2+i+k+j-1}{j}\pi_i \times\frac{G^{\lambda(\alpha_1+\alpha_2+i+k-1)+\lambda j}(x_2;\eta)}{(1-G(x_2;\eta))^{\lambda(\alpha_1+\alpha_2+i+k)+\lambda j+1}}$$

$$= g(x_2;\eta)\sum_{i,k,j,p=0}^{\infty}\Omega_{i,k,j,p}G^{\lambda(\alpha_1+\alpha_2+i+k-1)+\lambda j+p}(x_2;\eta)$$

$$= \sum_{i,k,j,p=0}^{\infty}\Omega_{i,k,j,p}\Phi_{i,k,j,p}(x_2;\eta), \tag{42}$$

where

$\Omega_{i,k,j,p} = \frac{\lambda(-1)^{k+j}\pi_i\binom{\beta-1}{k}}{B(\alpha_2,\beta)B(\alpha_1,\beta)}\binom{\alpha_1+\alpha_2+i+k+j-1}{j}\binom{\lambda(\alpha_1+\alpha_2+i+k)+\lambda j+p}{p}$

and

$\Phi_{i,k,j,p}(x_2;\eta) = g(x_2;\eta)G^{\lambda(\alpha_1+\alpha_2+i+k-1)+\lambda j+p}(x_2;\eta)$.

Substituting (42) into (39) yields the expression for the stress-strength reliability of the NBP-G family:

$$R = \sum_{i,k,j,p=0}^{\infty}\Omega_{i,k,j,p}\int_{-\infty}^{\infty}\Phi_{i,k,j,p}(x_2;\eta)dx_2. \tag{43}$$

3.5. Order statistics

Order statistics descry be the statistical properties of ranked observations in a sample. For the NBP-G family, the probability density function of the i^{th} order statistics is derived as:

$$f_{l,n}(x) = \frac{n! f(x) F(x)^{l-1}}{(l-1)!(n-l)!}\{1-F(x)\}^{n-l}, \tag{44}$$

where $F(x)$ and $f(x)$ are the CDF and PDF of the NBP-G family, respectively.

By applying (15), then (44) gives:

$$f_{l,n}(x) = f(x)\sum_{k=0}^{\infty}\Psi_k F(x)^{k+l-1}, \tag{45}$$

where $\Psi_k = \frac{n!(-1)^k\binom{n-l}{k}}{(l-1)!(n-l)!}$.

Substituting (9), then (45) gives:

$$f_{l,n}(x) = f(x)\sum_{k=0}^{\infty}\Psi_k\left\{\frac{\Delta^{\alpha}}{B(\alpha,\beta)}\sum_{i=0}^{\infty}\pi_i\Delta^i\right\}^{k+l-1}. \tag{46}$$

According to Biazatti et al. (Biazatti et al., 2022) and Gradshteyn and Ryzhik (Gradshteyn & Ryzhik, 1980), the power series expansion for $\left(\sum_{i=0}^{\infty}\pi_i\Delta^i\right)^{\nu}$ can be expressed as:

$$\left(\sum_{i=0}^{\infty}\pi_i\Delta^i\right)^{\nu} = \sum_{i=0}^{\infty}c_i^{(\nu)}\Delta^i, \tag{47}$$

where $c_0^{(\nu)} = \pi_0^{\nu}$ and $c_i^{(\nu)} = \frac{1}{i\pi_0}\sum_{m=1}^{i}\{(\nu+1)m-i\}.\pi_m c_{i-m}^{(\nu)}$, for $i \geq 1$. Using (47), then (46) can be reduced to:

$$f_{l,n}(x) = f(x)\sum_{k=0}^{\infty}\Psi_k\left\{\frac{\Delta^{\alpha}}{B(\alpha,\beta)}\right\}^{\nu}\sum_{i=0}^{\infty}c_i^{(\nu)}\Delta^i$$

$$= f(x)\sum_{k,i=0}^{\infty}\frac{\Psi_k c_i^{(\nu)}}{\{B(\alpha,\beta)\}^{\nu}}\frac{\left\{\left(\frac{G(x;\eta)}{1-G(x;\eta)}\right)^{\lambda}\right\}^{i+\alpha\nu}}{\left\{1+\left(\frac{G(x;\eta)}{1-G(x;\eta)}\right)^{\lambda}\right\}^{i+\alpha\nu}}, \tag{48}$$

where $\nu = k+l-1$. Substituting (7), then (48) can further be simplified as:

$$f_{l,n}(x) = \frac{\lambda g(x;\eta)G^{\lambda-1}(x;\eta)}{B(\alpha,\beta)(1-G(x;\eta))^{\lambda+1}}\sum_{k=0}^{\infty}$$

$$\times\sum_{i=0}^{\infty}\Psi_k\frac{c_i^{(\nu)}}{\{B(\alpha,\beta)\}^{\nu}}\frac{\left\{\left(\frac{G(x;\eta)}{1-G(x;\eta)}\right)^{\lambda}\right\}^{i+\alpha\nu+\alpha-1}}{\left\{1+\left(\frac{G(x;\eta)}{1-G(x;\eta)}\right)^{\lambda}\right\}^{2+i+\alpha\nu+\alpha-1}}$$

$$\times\left(1-\left(\frac{\left(\frac{G(x;\eta)}{1-G(x;\eta)}\right)^{\lambda}}{1+\left(\frac{G(x;\eta)}{1-G(x;\eta)}\right)^{\lambda}}\right)\right)^{\beta-1}. \tag{49}$$

Applying (15) into (49) yields:

$$f_{l,n}(x) = \frac{\lambda g(x;\eta)}{B(\alpha,\beta)}\sum_{k,i,p=0}^{\infty}\frac{(-1)^p\Psi_k c_i^{(\nu)}}{\{B(\alpha,\beta)\}^{\nu}}\frac{\binom{\beta-1}{p}\{G(x;\eta)\}^{\lambda-1+\lambda(i+\alpha\nu+\alpha+p-1)}}{\{1-G(x;\eta)\}^{\lambda+1+\lambda(i+\alpha\nu+\alpha+p-1)}\left\{1+\left(\frac{G(x;\eta)}{1-G(x;\eta)}\right)^{\lambda}\right\}^{2+i+\alpha\nu+\alpha+p-1}}$$

$$= \frac{\lambda g(x;\eta)}{B(\alpha,\beta)}\sum_{k,i,p,j=0}^{\infty}\frac{(-1)^{p+j}\Psi_k c_i^{(\nu)}}{\{B(\alpha,\beta)\}^{\nu}}\frac{\binom{\beta-1}{p}\binom{i+\alpha\nu+\alpha+p+j}{j}\{G(x;\eta)\}^{\lambda(i+\alpha\nu+\alpha+p)+\lambda j-1}}{\{1-G(x;\eta)\}^{\lambda(i+\alpha\nu+\alpha+p)+\lambda j+1}}$$

$$= \sum_{k,i,p,j,q=0}^{\infty}\Phi_{k,i,p,j,q}\Lambda_{k,i,p,j,q}(x;\eta), \tag{50}$$

where $\Phi_{k,i,p,j,q} = \frac{\lambda(-1)^{p+j}\Psi_k c_i^{(\nu)}}{\{B(\alpha,\beta)\}^{1+\nu}}\binom{\beta-1}{p}\binom{i+\alpha\nu+\alpha+p+j}{j}\binom{\lambda(i+\alpha\nu+\alpha+p)+\lambda j+q}{q}$ and $\Lambda_{k,i,p,j,q}(x;\eta) = g(x;\eta)\{G(x;\eta)\}^{\lambda(i+\alpha\nu+\alpha+p)+\lambda j+q-1}$.

4. Parameter estimation using MLE

Parameter estimation for the NBP-G family of distributions is performed using the MLE method. Given a random sample of n independent and identically distributed (i.i.d.) observations, $x_1, x_2, \ldots, x_n$, from the NBP-G distribution with parameters $\alpha, \beta, \lambda,$ and η, the likelihood function based on the PDF in (7) is given by:

$$\ell = \left(\frac{\lambda}{B(\alpha,\beta)}\right)^n\prod_{i=1}^{n}\left(\frac{g(x_i;\eta)G^{\lambda-1}(x_i;\eta)}{(1-G(x_i;\eta))^{\lambda+1}}\frac{w^{\alpha-1}(x_i;\lambda,\eta)(1-w(x_i;\lambda,\eta))^{\beta-1}}{\left\{1+\left(\frac{G(x_i;\eta)}{1-G(x_i;\eta)}\right)^{\lambda}\right\}^2}\right). \tag{51}$$

The corresponding log-likelihood function is expressed as:

$$L = n\log(\lambda) + n\log\left(\frac{\Gamma(\alpha+\beta)}{\Gamma(\alpha)\Gamma(\beta)}\right) + \sum_{i=1}^{n}(\log(g(x_i;\eta)))$$

$$+(\lambda-1)\sum_{i=1}^{n}(\log(G(x_i;\eta)))$$

$$+(\alpha-1)\sum_{i=1}^{n}(\log(w(x_i;\lambda,\eta))) + (\beta-1)\sum_{i=1}^{n}(\log(1-w(x_i;\lambda,\eta)))$$

$$-(\lambda+1)\sum_{i=1}^{n}(\log(1-G(x_i;\eta))) - 2\sum_{i=1}^{n}\left(\log\left(\left\{1+\left(\frac{G(x_i;\eta)}{1-G(x_i;\eta)}\right)^{\lambda}\right\}\right)\right), \tag{52}$$

where $\frac{1}{B(\alpha,\beta)} = \frac{\Gamma(\alpha+\beta)}{\Gamma(\alpha)\Gamma(\beta)}$ and $w(x_i;\lambda,\eta) = \frac{\left(\frac{G(x_i;\eta)}{1-G(x_i;\eta)}\right)^{\lambda}}{1+\left(\frac{G(x_i;\eta)}{1-G(x_i;\eta)}\right)^{\lambda}}$.

To determine the maximum likelihood estimates (MLEs) of the parameters, we compute the partial derivatives of the log-likelihood function with respect to each parameter $\alpha, \beta, \lambda,$ and η. The partial derivatives with respect to λ can be computed as:

$$\frac{\partial L}{\partial\lambda} = \frac{n}{\lambda} + \sum_{i=1}^{n}(\log(G(x_i;\eta)))$$

$$+(\alpha-1)\sum_{i=1}^{n}\left(\frac{\left\{\frac{G(x_i;\eta)}{1-G(x_i;\eta)}\right\}^{\lambda}\log\left(\frac{G(x_i;\eta)}{1-G(x_i;\eta)}\right)}{\left(1+\left\{\frac{G(x_i;\eta)}{1-G(x_i;\eta)}\right\}^{\lambda}\right)^2 w(x_i;\lambda,\eta)}\right)$$

Table 1
Behavior of the NBP-Weibull distribution PDF and hazard function.

x	α	β	θ	b	λ	PDF	Hazard
0.111837	1.1	1.5	2.1	0.5	0.1	0.042707224	0.111056280
0.213673	1.1	1.5	2.1	0.5	0.1	0.014519395	0.039103983
0.315510	1.1	1.5	2.1	0.5	0.1	0.007003435	0.019317383
0.417347	1.1	1.5	2.1	0.5	0.1	0.003960634	0.011131779
0.519184	1.1	1.5	2.1	0.5	0.1	0.002458539	0.007020302
0.621020	1.1	1.5	2.1	0.5	0.1	0.001623710	0.004701274
0.722857	1.1	1.5	2.1	0.5	0.1	0.001121264	0.003287255
0.824694	1.1	1.5	2.1	0.5	0.1	0.000800942	0.002375112
0.926531	1.1	1.5	2.1	0.5	0.1	0.000587598	0.001760993
1.028367	1.1	1.5	2.1	0.5	0.1	0.000440518	0.001333343
1.130204	1.1	1.5	2.1	0.5	0.1	0.000336246	0.001027291
1.232041	1.1	1.5	2.1	0.5	0.1	0.000260591	0.000803243
1.333878	1.1	1.5	2.1	0.5	0.1	0.000204614	0.000636063
1.435714	1.1	1.5	2.1	0.5	0.1	0.000162498	0.000509256
1.537551	1.1	1.5	2.1	0.5	0.1	0.000130348	0.000411698
1.639388	1.1	1.5	2.1	0.5	0.1	0.000105490	0.000335703
1.741224	1.1	1.5	2.1	0.5	0.1	8.60522E-05	0.000275849
1.843061	1.1	1.5	2.1	0.5	0.1	7.07001E-05	0.000228242
1.944898	1.1	1.5	2.1	0.5	0.1	5.84646E-05	0.000190042
2.046735	1.1	1.5	2.1	0.5	0.1	4.86332E-05	0.000159144
2.148571	1.1	1.5	2.1	0.5	0.1	4.06747E-05	0.000133971
2.250408	1.1	1.5	2.1	0.5	0.1	3.41885E-05	0.000113326
2.352245	1.1	1.5	2.1	0.5	0.1	2.88692E-05	9.62911E-05
2.454082	1.1	1.5	2.1	0.5	0.1	2.44819E-05	8.21562E-05
2.555918	1.1	1.5	2.1	0.5	0.1	2.08440E-05	7.03667E-05
2.657755	1.1	1.5	2.1	0.5	0.1	1.78126E-05	6.04861E-05
2.759592	1.1	1.5	2.1	0.5	0.1	1.52751E-05	5.21682E-05
2.861429	1.1	1.5	2.1	0.5	0.1	1.31418E-05	4.51366E-05
2.963265	1.1	1.5	2.1	0.5	0.1	1.13412E-05	3.91690E-05
3.065102	1.1	1.5	2.1	0.5	0.1	9.81560E-06	3.40858E-05

$$+(\beta-1)\sum_{i=1}^{n}\left(\frac{-\left\{\frac{G(x_i;\eta)}{1-G(x_i;\eta)}\right\}^{\lambda}\log\left(\left\{\frac{G(x_i;\eta)}{1-G(x_i;\eta)}\right\}\right)}{\left(1+\left\{\frac{G(x_i;\eta)}{1-G(x_i;\eta)}\right\}^{\lambda}\right)^{2}(1-w(x_i;\lambda,\eta))}\right)$$
$$-\sum_{i=1}^{n}(\log(1-G(x_i;\eta)))$$
$$-2\sum_{i=1}^{n}\left(\frac{\left(\frac{G(x_i;\eta)}{1-G(x_i;\eta)}\right)^{\lambda}\log\left(\frac{G(x_i;\eta)}{1-G(x_i;\eta)}\right)}{1+\left(\frac{G(x_i;\eta)}{1-G(x_i;\eta)}\right)^{\lambda}}\right). \quad (53)$$

The partial derivatives with respect to α can be computed as:

$$\frac{\partial L}{\partial\alpha}=n[\psi(\alpha,\beta)]_{\alpha}-n[\psi(\alpha)]+\sum_{i=1}^{n}(\log(w(x_i;\lambda,\eta))), \quad (54)$$

where $[\psi(\alpha)]=\frac{1}{\Gamma(\alpha)}\frac{\partial}{\partial\alpha}\{\Gamma(\alpha)\}=\frac{[\Gamma'(\alpha)]}{\Gamma(\alpha)}$ and $[\psi(\alpha,\beta)]_{\alpha}=\frac{1}{\Gamma(\alpha+\beta)}\frac{\partial}{\partial\alpha}\{\Gamma(\alpha+\beta)\}=\frac{[\Gamma'(\alpha+\beta)]_{\alpha}}{\Gamma(\alpha+\beta)}$.

The partial derivatives with respect to β can be computed as:

$$\frac{\partial L}{\partial\beta}=-n[\psi(\alpha,\beta)]_{\beta}-n[\psi(\alpha)]+\sum_{i=1}^{n}(\log(1-w(x_i;\lambda,\eta))), \quad (55)$$

where $[\psi(\beta)]=\frac{1}{\Gamma(\beta)}\frac{\partial}{\partial\beta}\{\Gamma(\beta)\}=\frac{[\Gamma'(\beta)]}{\Gamma(\beta)}$ and $[\psi(\alpha,\beta)]_{\beta}=\frac{1}{\Gamma(\alpha+\beta)}\frac{\partial}{\partial\beta}\{\Gamma(\alpha+\beta)\}=\frac{[\Gamma'(\alpha+\beta)]_{\beta}}{\Gamma(\alpha+\beta)}$.

Finally, the partial derivatives with respect to η can be computed as:

$$\frac{\partial L}{\partial\eta}=\sum_{i=1}^{n}\left(\frac{[g'(x_i;\eta)]_{\eta}}{g(x_i;\eta)}\right)+(\lambda-1)\sum_{i=1}^{n}\left(\frac{G'(x_i;\eta)}{G(x_i;\eta)}\right)+(\alpha-1)\sum_{i=1}^{n}\left(\frac{w'(x_i;\lambda,\eta)}{w(x_i;\lambda,\eta)}\right)$$
$$-(\beta-1)\sum_{i=1}^{n}\left(\frac{w'(x_i;\lambda,\eta)}{1-w(x_i;\lambda,\eta)}\right)$$
$$+(\lambda+1)\sum_{i=1}^{n}\left(\frac{G'(x_i;\eta)}{1-G(x_i;\eta)}\right)-2$$
$$\times\sum_{i=1}^{n}\left(\frac{\lambda G'(x_i;\eta)\left(\frac{G(x_i;\eta)}{1-G(x_i;\eta)}\right)^{\lambda-1}}{(1-G(x_i;\eta))^{2}\left(1+\left(\frac{G(x_i;\eta)}{1-G(x_i;\eta)}\right)^{\lambda}\right)}\right), \quad (56)$$

where $\frac{\partial}{\partial\eta}\{g(x_i;\eta)\}=[g'(x_i;\eta)]_{\eta}$ and $\frac{\partial}{\partial\eta}\{G(x_i;\eta)\}=G'(x_i;\eta)$.

Equating (53)-(56) to zero and solving these equations simultaneously yields the MLEs for the parameters of the NBP-G family. Since these equations are generally nonlinear, numerical optimization methods such as Newton-Raphson are often required to compute the estimates. Parameter estimation was performed using the Newton-Raphson algorithm with a convergence tolerance set to 10^{-6}. All computations were implemented in R.

5. Development of the New Beta Prime-Weibull distribution

The New Beta Prime-Weibull (NBP-Weibull) distribution is constructed by combining the NBP-G family with the Weibull distribution as the baseline model. The CDF of the NBP-Weibull distribution is obtained by substituting the Weibull CDF defined in (2) into the CDF of the NBP-G family in (6):

$$F(x;\alpha,\beta,\lambda,\theta,b)=\frac{B_y(\alpha,\beta)}{B(\alpha,\beta)};\quad x>0;\quad \alpha,\beta,\lambda,\theta,b>0, \quad (57)$$

where $y=\frac{\left(\frac{1-e^{-\theta x^{b}}}{e^{-\theta x^{b}}}\right)^{\lambda}}{1+\left(\frac{1-e^{-\theta x^{b}}}{e^{-\theta x^{b}}}\right)^{\lambda}}$ $\alpha,\beta,$ and θ are shape parameters, λ is an exponent parameter, and b is a scale parameter.

To derive the PDF for the NBP-Weibull distribution, the PDF in (1) and the corresponding Weibull CDF in (2) are substituted into the PDF of the NBP-G family defined in (7):

$$f(x)=\frac{\lambda\theta b x^{b-1}}{B(\alpha,\beta)\left(e^{-\theta x^{b}}\right)^{\lambda\alpha}}\frac{\left(1-e^{-\theta x^{b}}\right)^{\lambda\alpha-1}}{\left\{1+\left(\frac{1-e^{-\theta x^{b}}}{e^{-\theta x^{b}}}\right)^{\lambda}\right\}^{\alpha+\beta}};\quad x>0;\quad \alpha,\beta,\lambda,\theta,b>0. \quad (58)$$

The survival, hazard, and quantile functions of the NBP-Weibull distribution are presented as:

$$S(x)=1-\frac{B_y(\alpha,\beta)}{B(\alpha,\beta)};\quad x>0;\quad \alpha,\beta,\lambda,\theta,b>0, \quad (59)$$

$$h(x)=\frac{\lambda\theta b x^{b-1}\left(1-e^{-\theta x^{b}}\right)^{\lambda\alpha-1}\left\{1+\left(\frac{1-e^{-\theta x^{b}}}{e^{-\theta x^{b}}}\right)^{\lambda}\right\}^{-(\alpha+\beta)}}{\left(e^{-\theta x^{b}}\right)^{\lambda\alpha}\{B(\alpha,\beta)-B_y(\alpha,\beta)\}};\quad x>0;\quad \alpha,\beta,\lambda,\theta,b>0, \quad (60)$$

and

$$x_q=\left\{-\frac{1}{\theta}\log\left\{1-\frac{\left\{\frac{I^{-1}(u,\alpha,\beta)}{1-I^{-1}(u,\alpha,\beta)}\right\}^{\frac{1}{\lambda}}}{1+\left\{\frac{I^{-1}(u,\alpha,\beta)}{1-I^{-1}(u,\alpha,\beta)}\right\}^{\frac{1}{\lambda}}}\right\}\right\}^{\frac{1}{b}}, \quad (61)$$

where $y=\frac{\left(\frac{1-e^{-\theta x^{b}}}{e^{-\theta x^{b}}}\right)^{\lambda}}{1+\left(\frac{1-e^{-\theta x^{b}}}{e^{-\theta x^{b}}}\right)^{\lambda}}$.

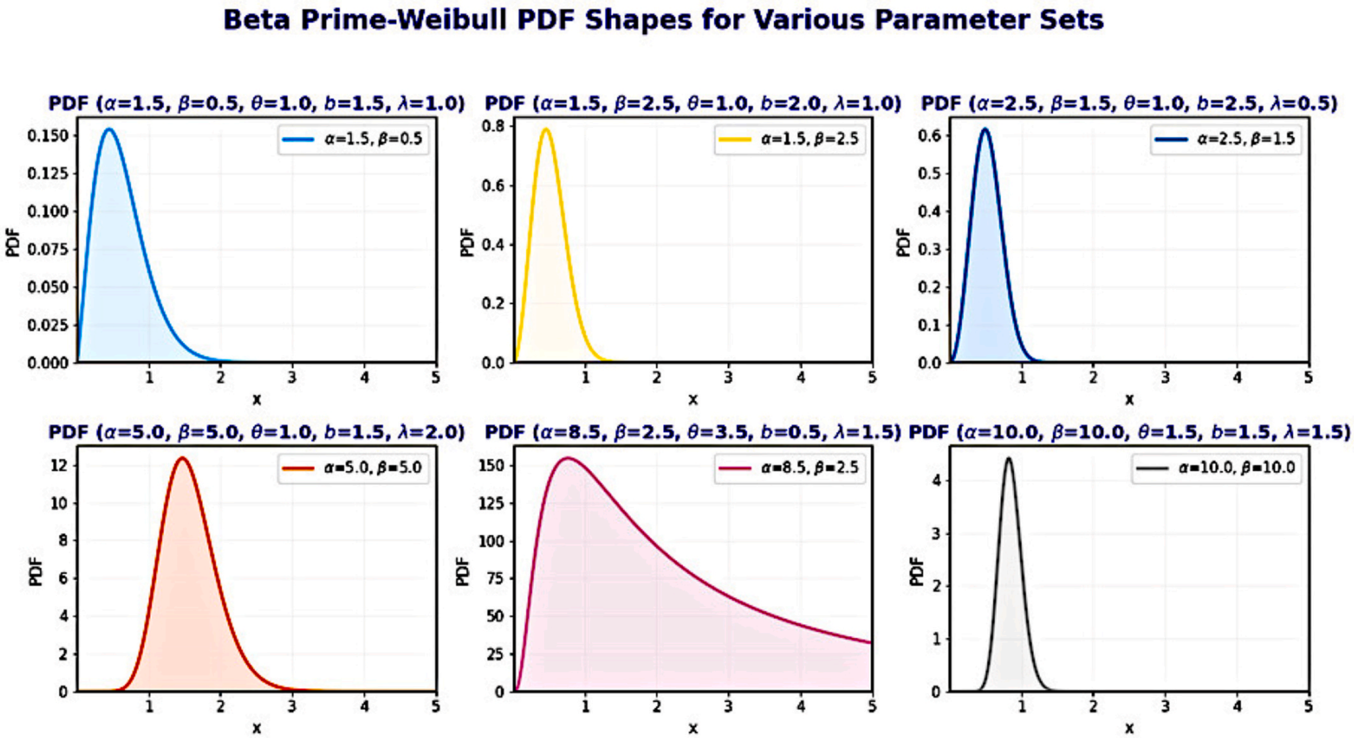

Fig. 2. Potential PDF shapes of the NBP-Weibull distribution.

5.1. Numerical and graphical behavior of the NBP-weibull distribution

This subsection presents the theoretical results of the NBP-Weibull model derived from the BP-G family. The focus is on the analytical and graphical properties of the NBP-Weibull distribution, including a detailed analysis of the PDF, hazard function, and key statistical properties such as mean, variance, skewness, and kurtosis. Additionally, numerical tables and visualizations provide further insights into the

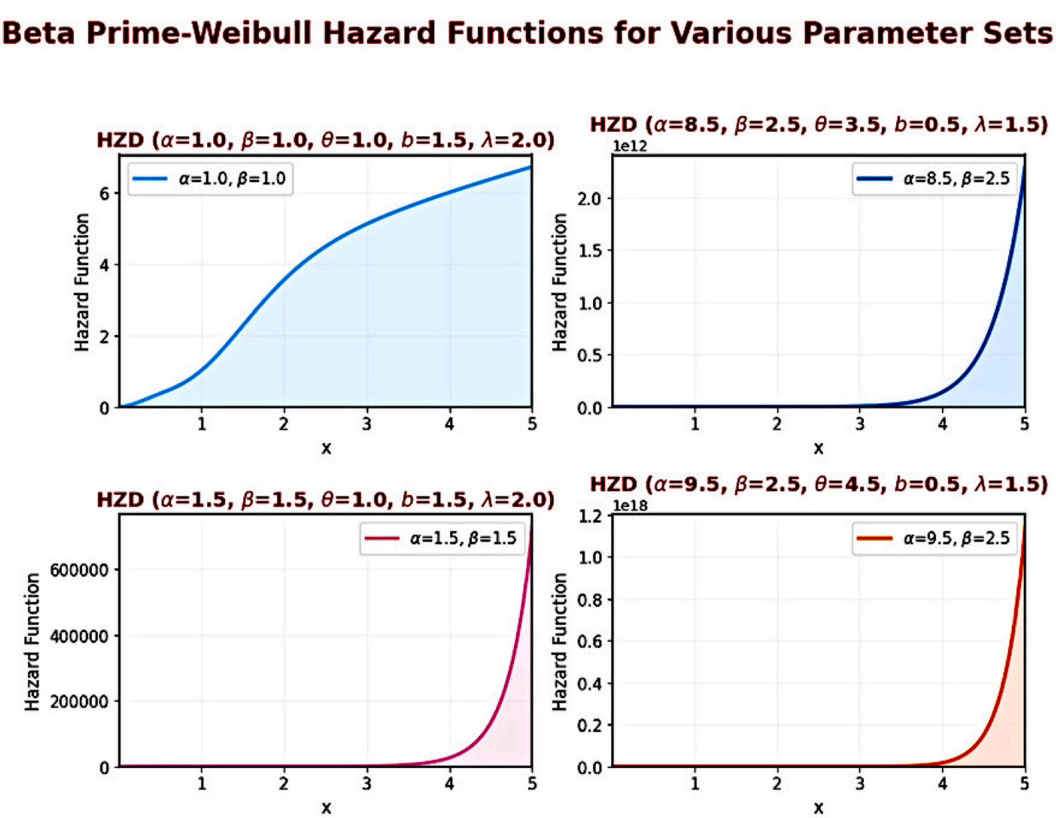

Fig. 3. Potential hazard function shapes of the NBP-Weibull distribution.

Table 2
Summary of statistical properties for the NBP-Weibull distribution.

α	β	θ	b	λ	Mean	Variance	Skewness	Kurtosis
1	1	0.5	0.5	0.5	4.67261	15.22941	−0.12486	−1.70755
1	2	0.5	0.5	0.5	3.27781	14.73325	0.52409	−1.49862
1	3	0.5	0.5	0.5	2.02352	11.21444	1.28666	−0.08523
1	4	0.5	0.5	0.5	1.12681	6.938230	2.25267	3.47380
1	5	0.5	0.5	0.5	0.58994	3.716710	3.55698	11.41247
1	6	0.5	0.5	0.5	0.30278	1.826430	5.38970	28.70421
1	7	0.5	0.5	0.5	0.15799	0.856280	8.01329	66.12672
1	8	0.5	0.5	0.5	0.08647	0.392130	11.78015	146.5463
1	9	0.5	0.5	0.5	0.05086	0.177930	17.13642	317.0410
1	10	0.5	0.5	0.5	0.03252	0.080810	24.57925	669.8278
2.5	1	0.5	0.5	0.5	4.62167	15.31869	−0.10166	−1.71866
2.5	2	0.5	0.5	0.5	3.21882	14.67192	0.55409	−1.46839
2.5	3	0.5	0.5	0.5	1.97165	11.03728	1.32712	0.02201
2.5	4	0.5	0.5	0.5	1.09035	6.757000	2.31037	3.74499
2.5	5	0.5	0.5	0.5	0.56780	3.590540	3.64273	12.05305
2.5	6	0.5	0.5	0.5	0.29030	1.754190	5.51989	30.18766
2.5	7	0.5	0.5	0.5	0.15111	0.818940	8.21224	69.52604
2.5	8	0.5	0.5	0.5	0.08261	0.373820	12.08323	154.2492
2.5	9	0.5	0.5	0.5	0.04859	0.169190	17.59328	334.2232
2.5	10	0.5	0.5	0.5	0.03109	0.076680	25.25552	707.2587
5	1	0.5	0.5	0.5	4.03097	15.96899	0.16904	−1.75335
5	2	0.5	0.5	0.5	2.59072	13.58331	0.90253	−0.97588
5	3	0.5	0.5	0.5	1.46485	9.020760	1.80076	1.52931
5	4	0.5	0.5	0.5	0.75860	4.984800	2.99209	7.46509
5	5	0.5	0.5	0.5	0.37677	2.461040	4.66152	20.81574
5	6	0.5	0.5	0.5	0.18681	1.142820	7.07007	50.52965
5	7	0.5	0.5	0.5	0.09570	0.514630	10.58202	116.3192
5	8	0.5	0.5	0.5	0.05221	0.22864	15.69174	260.7357
5	9	0.5	0.5	0.5	0.03103	0.101280	23.02887	572.7685
5	10	0.5	0.5	0.5	0.02024	0.045100	33.29274	1228.887
7.5	1	0.5	0.5	0.5	3.08414	15.41896	0.63292	−1.42441
7.5	2	0.5	0.5	0.5	1.76231	10.85953	1.50689	0.48657
7.5	3	0.5	0.5	0.5	0.90276	6.141000	2.64625	5.36922
7.5	4	0.5	0.5	0.5	0.43588	3.030170	4.23862	16.72881
7.5	5	0.5	0.5	0.5	0.20716	1.389590	6.55198	42.71121
7.5	6	0.5	0.5	0.5	0.10045	0.614650	9.96964	101.8494
7.5	7	0.5	0.5	0.5	0.05136	0.267500	15.03447	235.6878
7.5	8	0.5	0.5	0.5	0.02854	0.115820	22.49092	535.4549
7.5	9	0.5	0.5	0.5	0.01756	0.050250	33.29009	1194.782
7.5	10	0.5	0.5	0.5	0.01197	0.022000	48.47221	2601.381
10	1	0.5	0.5	0.5	2.05573	12.59384	1.27384	−0.21088

behavior and adaptability of the proposed NBP-Weibull model for diverse applications.

Table 1 presents the behavior of the NBP-Weibull distribution with varying parameter values of $\alpha = 1.1, \beta = 1.5, \theta = 2.1, b = 0.5,$ and $\lambda = 0.1$. The table demonstrates how the PDF and hazard rate evolve as the value of x increases. For smaller values of α and β, both the PDF and hazard rate are initially high, indicating a greater likelihood of an event (or failure) occurring early. As α and β increase, both the PDF and the hazard rate decline much more rapidly, suggesting that the probability of an event diminishes quickly over time. This trend is evident in the steep decline from high initial values toward nearly zero as x progresses.

Fig. 2 illustrates the potential shapes of the NBP–Weibull distribution's PDF, highlighting its flexibility. The plots display a variety of forms depending on parameter combinations. For example, with $\alpha = 1.5, \beta = 0.5, \theta = 1.0, b = 1.5,$ and $\lambda = 1.0$, the PDF is sharply right-skewed with a tall peak near zero that decays rapidly, capturing highly skewed data. In contrast, with $\alpha = 5.0, \beta = 5.0, \theta = 1.0, b = 1.5,$ and $\lambda = 2.0$, the distribution is nearly symmetric with a bell-shaped form, showing that the model can also represent balanced data. When $\alpha = 10.0, \beta = 10.0, \theta = 1.5, b = 1.5,$ and $\lambda = 1.5$, the PDF is also symmetric but narrower and more concentrated around the mean. These results confirm that the NBP–Weibull distribution can flexibly represent both skewed and symmetric datasets depending on the parameter settings.

Fig. 3 presents the hazard rate functions of the BP–Weibull distribution for different parameter sets. In the top-left panel ($\alpha = 1.0, \beta = 1.0, \theta = 1.0, b = 1.5, \lambda = 2.0$), the hazard function shows an increasing hazard rate**,** where the risk of failure rises steadily as x increases. In the top-right panel ($\alpha = 8.5, \beta = 2.5, \theta = 3.5, b = 0.5, \lambda = 1.5$), the hazard rate stays low at first and then increases rapidly for larger values of x. In the bottom-left panel ($\alpha = 1.5, \beta = 1.5, \theta = 1.0, b = 1.5, \lambda = 2.0$), the hazard function grows very quickly after $x = 4$, representing a sharply increasing hazard rate. Finally, in the bottom-right panel ($\alpha = 9.5, \beta = 2.5, \theta = 4.5, b = 0.5, \lambda = 1.5$), the hazard function is nearly flat at small x values, but then increases extremely fast as x becomes large. These results demonstrate that the NBP–Weibull distribution is sufficiently flexible to represent various types of increasing hazard rates, which is crucial in reliability, biomedical, and engineering applications.

The parameters $\alpha, \beta, \lambda,$ and η play distinct roles in shaping the distribution. The shape parameters α and β primarily control skewness and tail behavior, allowing the distribution to transition between left-skewed, right-skewed, and near-symmetric forms. The exponent parameter λ influences the rate of decay and overall curvature of the distribution, affecting both the density and hazard function. The scale parameter η governs the spread of the distribution and determines the scale of the data. Together, these parameters provide substantial flexibility in modeling complex real-world data.

The graphical analysis confirms that the NBP-Weibull distribution can exhibit increasing, rapidly increasing, and near-constant hazard rate patterns depending on parameter configurations. This flexibility is essential for modeling radiation exposure and reliability data where failure mechanisms evolve.

Table 2 provides insights into the mean, variance, skewness, and kurtosis of the NBP-Weibull distribution. It highlights how these characteristics vary across different parameter combinations. The mean and

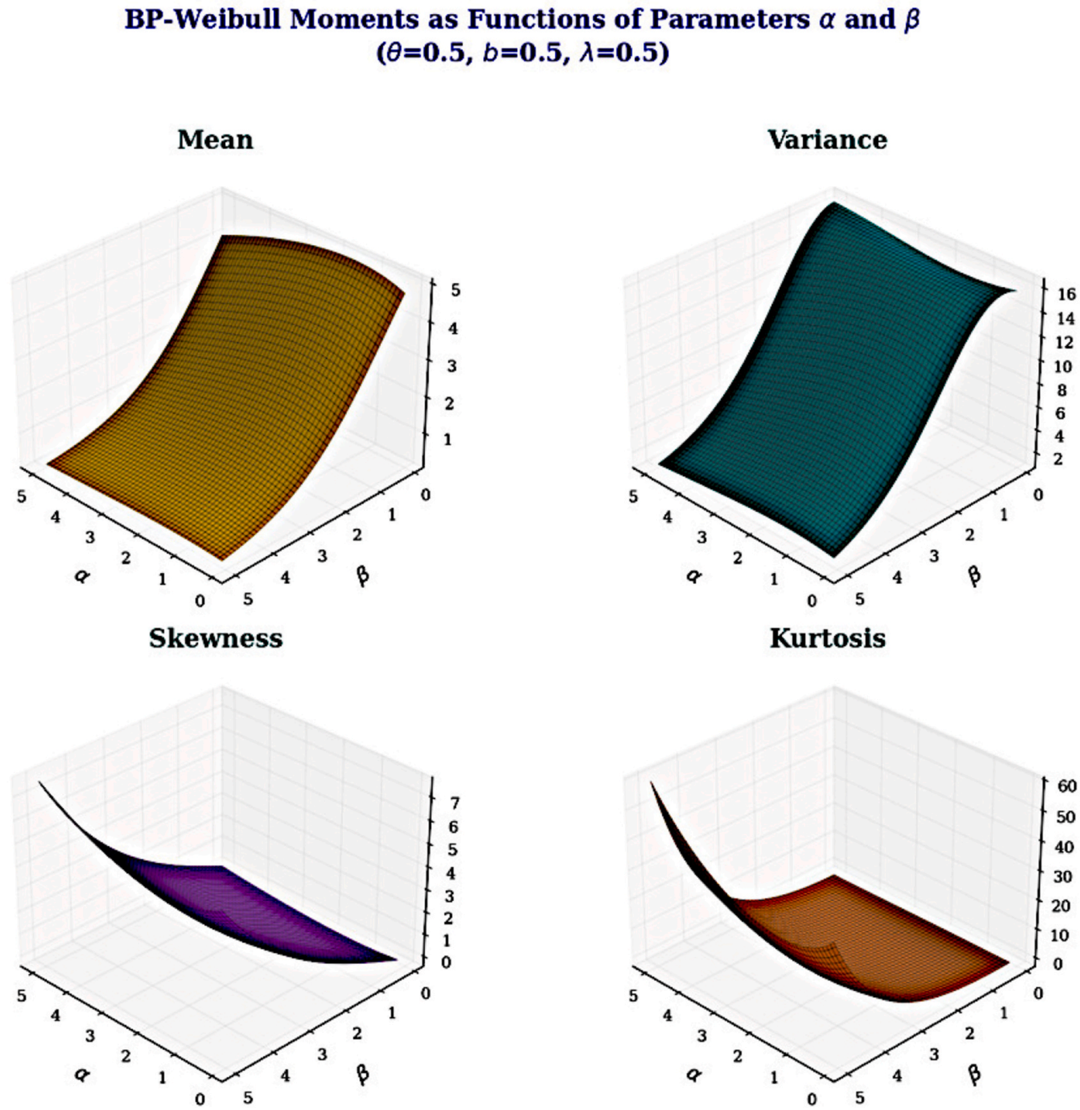

Fig. 4. 3D moments plots for the NBP-Weibull distribution.

variance vary significantly with different parameters. This shows the distribution's ability to capture a wide range of central tendencies and dispersions. For a fixed α, increasing the value of β leads to a significant decrease in both the mean and the variance. For instance, with $\alpha = 1$, increasing β from 1 to 10 causes the mean to drop from 4.67261 to 0.03252 and the variance to decrease from 15.22941 to 0.08081. Similarly, as α increases (with a fixed β), a similar decreasing trend is observed for both the mean and variance. This inverse relationship demonstrates the model's ability to adapt to data.

The skewness values highlight the model's ability to capture both right-skewed and left-skewed data distributions. For a fixed value of α, as β increases, the skewness transitions from a negative to a positive value. For example, when $\alpha = 1$, the skewness value is -0.12486 at $\beta = 1$ (indicating a slight left skew) but dramatically increases to 24.57925 at $\beta = 10$ (indicating a strong right skew). This pattern is consistent across the various α values tested.

Kurtosis, which reflects the distribution's peak and tail behavior, also varies significantly. For a fixed α, increasing β leads to a noticeable increase in the kurtosis. At lower values of β, the kurtosis is negative (e.g., -1.70755 for $\alpha = 1, \beta = 1$), suggesting a platykurtic distribution with a flatter peak and lighter tails compared to a normal distribution. However, as β increases, the kurtosis becomes positive and grows significantly (e.g., 669.8278 for $\alpha = 1$, $\beta = 10$), indicating a leptokurtic distribution with a much sharper peak and heavier tails. This responsiveness to parameter changes allows the NBP-Weibull model to accurately fit data with different tail behaviors. The visual representations of these moments in Fig. 4 confirm the sensitivity of the distribution's characteristics to changes in the parameters α and β. This makes the NBP-Weibull model a valuable choice for analyzing diverse datasets in practical applications.

The observation that the variance exceeds the mean is indicative of over-dispersion, a common feature in radiation data due to inherent variability and uncertainty in exposure processes. Rather than indicating instability, this behavior demonstrates the flexibility of the model in capturing complex data structures that deviate from classical assumptions.

6. Monte Carlo simulation study

A Monte Carlo simulation study was conducted to evaluate the performance of the MLE method for the NBP-Weibull distribution. The simulation study was designed to assess the accuracy and reliability of the MLE method in estimating the parameters of the NBP-Weibull distribution. The Monte Carlo simulation study was conducted using 1000 replications for each sample size. Sample sizes of $n = 50, 100, 200,$ and 500 were considered. Parameter estimation was performed using nu-

Table 3
Monte Carlo simulation results for the NBP-Weibull distribution for Case 1 and Case 2.

n	Case 1 $\alpha = 1.5, \beta = 2.5, \theta = 1.2, b = 0.8, \lambda = 1.0$				Case 2 $\alpha = 2.0, \beta = 3.0, \theta = 1.5, b = 1.2, \lambda = 2.0$		
	Estimate	Mean	Bias	MSE	Mean	Bias	MSE
50	$\hat{\alpha}$	1.482	−0.018	0.035	1.973	−0.027	0.051
	$\hat{\beta}$	2.492	−0.008	0.056	2.984	−0.016	0.073
	$\hat{\theta}$	1.184	−0.016	0.031	1.482	−0.018	0.041
	$\hat{b}$	0.794	−0.006	0.014	1.194	−0.006	0.026
	$\hat{\lambda}$	1.021	0.021	0.021	2.021	0.021	0.031
100	$\hat{\alpha}$	1.493	−0.007	0.019	1.993	−0.007	0.029
	$\hat{\beta}$	2.506	0.006	0.034	2.996	−0.004	0.045
	$\hat{\theta}$	1.195	−0.005	0.019	1.494	−0.004	0.045
	$\hat{b}$	0.802	0.002	0.008	1.201	0.001	0.017
	$\hat{\lambda}$	1.011	0.011	0.014	2.011	0.011	0.022
200	$\hat{\alpha}$	1.498	−0.002	0.010	1.998	−0.002	0.020
	$\hat{\beta}$	2.504	0.004	0.021	3.003	0.003	0.031
	$\hat{\theta}$	1.198	−0.002	0.011	1.498	−0.002	0.018
	$\hat{b}$	0.801	0.001	0.005	1.200	0.000	0.012
	$\hat{\lambda}$	1.006	0.006	0.009	2.006	0.006	0.016
500	$\hat{\alpha}$	1.499	−0.001	0.004	2.000	0.000	0.012
	$\hat{\beta}$	2.503	0.003	0.013	3.001	0.001	0.019
	$\hat{\theta}$	1.199	−0.001	0.006	1.500	0.000	0.007
	$\hat{b}$	0.800	0.000	0.003	1.200	0.000	0.007
	$\hat{\lambda}$	1.003	0.003	0.005	2.003	0.003	0.010

merical optimization via the Newton-Raphson algorithm implemented in the R software. For each sample size, 1000 random samples were generated from the NBP-Weibull distribution, and the parameters were estimated using the MLE method. Two cases were considered:

Case 1. $\alpha = 1.5, \beta = 2.5, \theta = 1.2, b = 0.8,$ and $\lambda = 1.0$

Case 2. $\alpha = 2.0, \beta = 3.0, \theta = 1.5, b = 1.2,$ and $\lambda = 2.0.$

The performance of the MLE method was evaluated using several criteria, including mean, Bias, and mean squared error (MSE). The simulation results for Case 1 and Case 2 are presented in Table 3. The table shows the average estimated values, means, biases, and MSEs for each parameter and sample size. The results indicate that the MLE method provides accurate and reliable estimates of the parameters of the NBP-Weibull distribution.

The results of the simulation study demonstrate the effectiveness of the MLE method in estimating the parameters of the NBP-Weibull distribution. The means, biases, and MSEs decrease as the sample size increases. The results also show that the MLE method demonstrates accurate and reliable estimates of the parameters of the NBP-Weibull distribution for different parameter values.

7. Application to radiation datasets

This section presents the analysis of real-world datasets using the proposed NBP-Weibull distribution. The primary objective is to validate the applicability, robustness, and flexibility of the new model in capturing complex patterns in diverse radiation datasets. The proposed NBP-Weibull distribution is applied to real-world data and evaluated for its performance. The NBP-Weibull model is compared against its well-established counterparts to assess its relative effectiveness. These comparisons are conducted using goodness-of-fit criteria, including the Akaike information criterion (AIC), Bayesian information criterion (BIC), Hannan-Quinn information criterion (HQIC), consistent Akaike information criterion (CAIC), and log-likelihood values. The model that achieves the lowest AIC, BIC, HQIC, and CAIC values, along with the highest log-likelihood, is considered better in modeling the dataset.

Table 4
Descriptive summaries for Data I-III.

Statistics	Data I	Data II	Data III
Minimum	1.265	1.395	1.261
First Quartile	1.338	1.527	1.456
Median	1.649	2.029	1.827
Mean	1.757	1.944	1.802
Third Quartile	2.050	2.236	2.085
Maximum	2.349	2.535	2.405
Std. Deviation	0.3741078	0.3729875	0.3655972
Skewness	0.1879781	−0.1852032	0.05051146
kurtosis	−1.426588	−1.448772	−1.335588

To demonstrate the applicability and performance of the proposed NBP-Weibull distribution, three distinct radiation real-world datasets were selected for analysis. The choice of the radiation datasets (Data I-III) is strategic, as they represent distinct data types with different statistical characteristics. This approach allows for demonstration of the proposed models' flexibility in accommodating various distributional shapes, including varying degrees of skewness and kurtosis.

7.1. Radiation data

The radiation data consists of three datasets, each representing the susceptibility index (SI) of unirradiated peppermint packets and irradiated with gamma rays or microwave rays to adult infestation of *Stegobium paniceum* L. The SI represents a quantitative measure of the resistance of materials to biological infestation following radiation exposure. It reflects the combined effects of radiation dose, exposure duration, and material properties. These datasets are particularly suitable for evaluating the proposed model due to their inherent variability, skewness, and complex reliability behavior.

7.1.1. Data I: non-choice packet test

The first dataset, Data I, comprises 21 observations of the SI of unirradiated peppermint packets irradiated with gamma rays (6, 8, 10 KGy) or microwave rays (1, 2, 3 min) to adult infestation of *Stegobium paniceum* L. under a non-choice packet test. The dataset is given as follows:

2.342985965, 2.349130571, 2.33606346, 2.049882604, 1.912952545, 2.158918912, 1.693929873, 1.603470002, 1.611406655, 1.328521137, 1.264520993, 1.311742231, 2.019587063, 2.08278537, 1.954249732, 1.621876146, 1.647866671, 1.649076005, 1.337911092, 1.337911092, 1.290128553.

This dataset was originally analyzed by Abdelfattah and Sayed (Abdelfattah & Sayed, 2022) to investigate the comparative efficacy of gamma and microwave radiation in protecting peppermint from infestation by drugstone beetle (*Stegobium paniceum*) L.

7.1.2. Data II: choice packet test

The second dataset, Data II, consists of 21 observations of the susceptibility index (SI) of unirradiated peppermint packets irradiated with gamma rays (6, 8, 10 KGy) or microwave rays (1, 2, 3 min) to adult infestation of *Stegobium paniceum* L. under the choice packet test. The dataset is given as follows:

2.463871049, 2.534601047, 2.342430823, 2.120520465, 2.235678759, 2.177037749, 1.79120227, 1.865753707, 1.754017205, 1.498275501, 1.411231151, 1.394837635, 2.287564493, 2.183200002, 2.252259207, 2.029383778, 2.096705442, 1.970275512, 1.526788015, 1.426894443, 1.452740448.

This dataset was also analyzed by Abdelfattah and Sayed (Abdelfattah & Sayed, 2022) to compare the efficacy of gamma and microwave radiation in protecting peppermint from infestation by drugstone beetle (*Stegobium paniceum*) L.

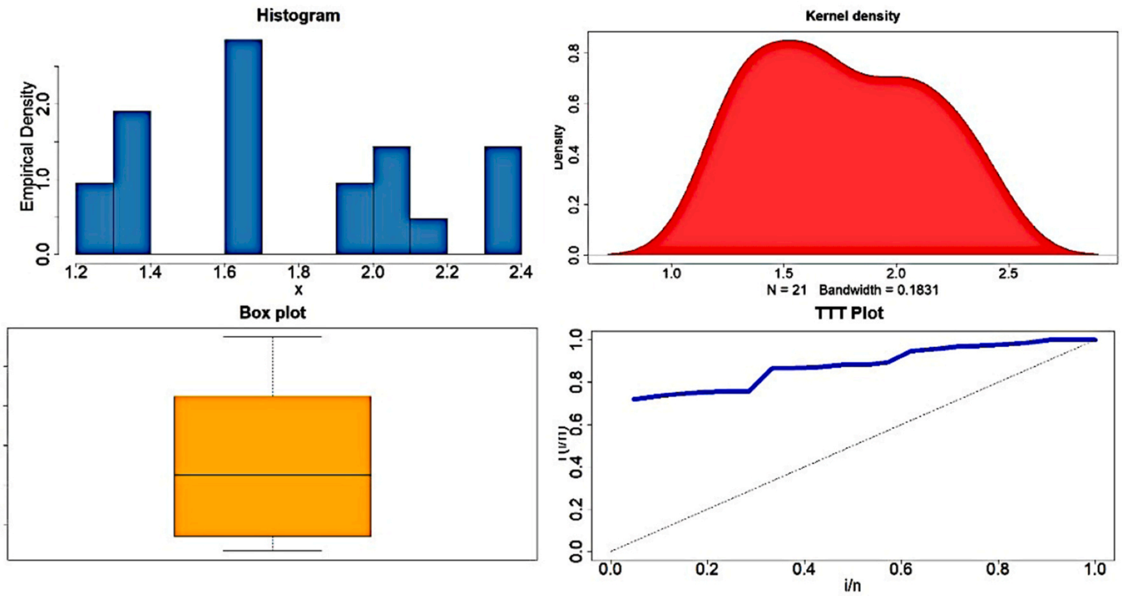

Fig. 5. Graphical representations of Data I.

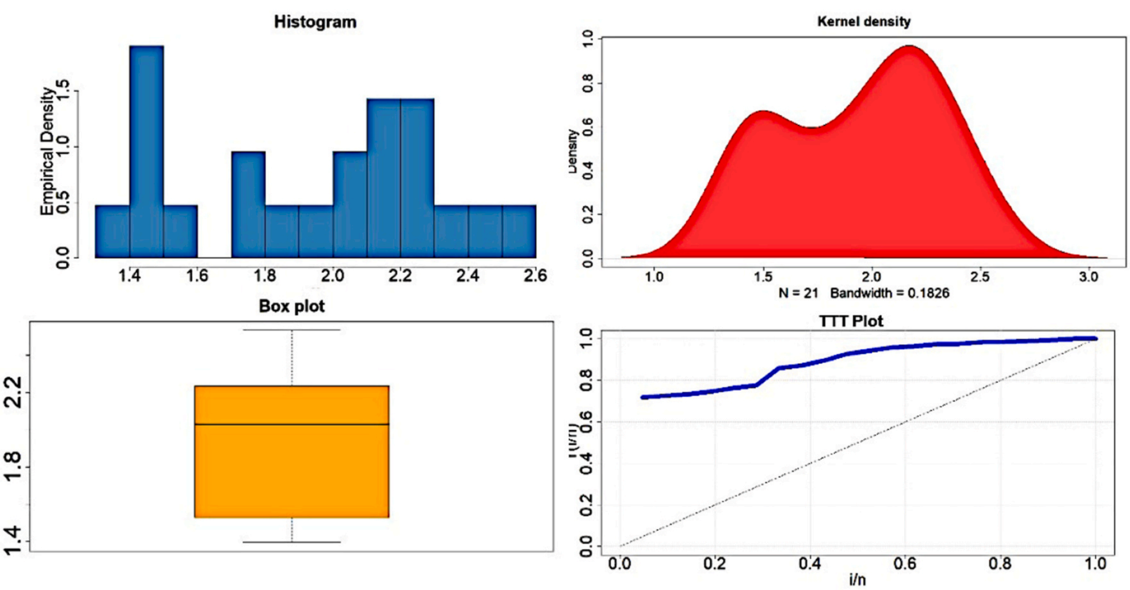

Fig. 6. Graphical representations of Data II.

7.1.3. Data III: choice non-packet test

The third dataset, Data III, comprises 21 observations of the susceptibility index (SI) of unirradiated peppermint packets irradiated with gamma rays (6, 8, 10 KGy) or microwave rays (1, 2, 3 min) to adult infestation of *Stegobium paniceum* L. under a choice non-packet test. The dataset is given as follows:

2.322974606, 2.355195374, 2.404551744, 1.963550292, 2.003252618, 1.892611657, 1.84509804, 1.791656596, 1.826829743, 1.279044486, 1.26146456, 1.310229519, 2.0853111, 2.144659472, 2.161135204, 1.705686555, 1.634019052, 1.581664341, 1.399 649181, 1.410499175, 1.455635148.

This dataset was also analyzed by Abdelfattah and Sayed (Abdelfattah & Sayed, 2022) to investigate the comparative efficacy of gamma and microwave radiation in protecting peppermint from infestation by drugstone beetle (*Stegobium paniceum*) L.

These datasets will be used to illustrate the application of the new NBP-Weibull model in modeling radiation data. The results will be compared with other existing models to demonstrate the adequacy of the proposed model.

7.2. Numerical and graphical representations of data I and data II

An initial analysis of the two datasets was performed to understand their basic statistical features. This initial assessment, which includes both numerical summaries and visual graphs, is essential for choosing the right probability distributions for future modeling. Table 4 presents the summary statistics for Data I-III, representing the susceptibility index of unirradiated peppermint packets and those irradiated with gamma rays or microwave rays to adult infestation of *Stegobium paniceum* L. The datasets exhibit distinct statistical properties.

Data I has a mean susceptibility index of 1.757, with a median of 1.649 and a standard deviation of 0.3741. The minimum and maximum

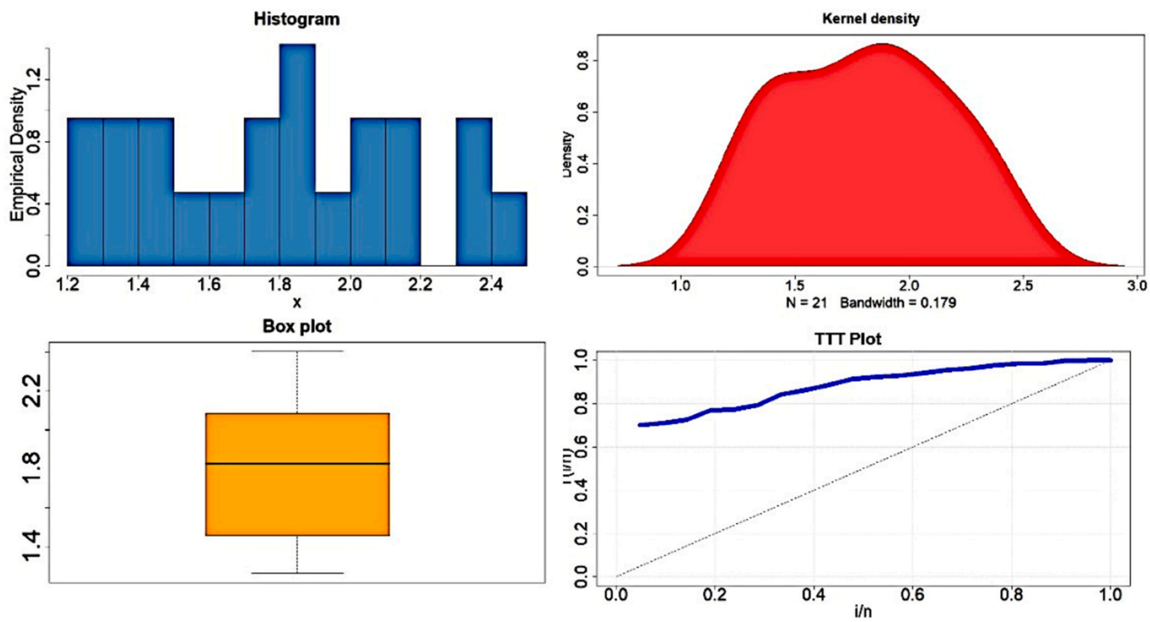

Fig. 7. Graphical representations of Data III.

Table 5
MLEs and evaluation metrics of the competitive models for Data 1.

Model	Estimate	L	AIC	CAIC	BIC	HQIC
BP-Weibull	$\widehat{b} = 2.1036$ $\widehat{\theta} = 1.5507$ $\widehat{\alpha} = 2.0866$ $\widehat{\beta} = 0.3341$ $\widehat{\lambda} = 1.9047$	**176.5572**	**−343.1143**	**−339.1143**	**−337.8917**	**−341.9809**
Weibull	$\widehat{b} = 0.0550$ $\widehat{\theta} = 4.6583$	−9.1749	22.3497	23.0164	24.4388	22.8031
M-Weibull	$\widehat{b} = 1.2325$ $\widehat{\theta} = 0.5132$ $\widehat{\nu} = 1.2451$	−9.0121	24.0242	25.4359	27.1577	24.7042
MO-Weibull	$\widehat{b} = 1.6036$ $\widehat{\theta} = 0.6295$ $\widehat{\omega} = 1.8872$	−18.5878	43.1755	44.5873	46.3091	43.8556
E-Weibull	$\widehat{b} = 1.6791$ $\widehat{\theta} = 0.6817$ $\widehat{\upsilon} = 1.9012$	−16.0610	38.1221	39.5338	41.2556	38.8021
MOD-Weibull	$\widehat{b} = 0.0467$ $\widehat{\theta} = 0.1983$ $\widehat{\delta} = 1.9919$	−121.8550	49.7109	51.1227	52.8445	50.3910

values are 1.265 and 2.349, respectively, indicating a relatively moderate spread of data points. The skewness of 0.188 suggests a slightly right-skewed distribution, while the kurtosis of −1.427 indicates a platykurtic distribution.

Data II exhibits a mean susceptibility index of 1.944, with a median of 2.029 and a standard deviation of 0.373. The minimum and maximum values are 1.395 and 2.535, respectively. The skewness of −0.185 suggests a slightly left-skewed distribution, while the kurtosis of −1.449 indicates a platykurtic distribution.

Data III has a mean susceptibility index of 1.802, with a median of 1.827 and a standard deviation of 0.3656. The minimum and maximum values are 1.261 and 2.405, respectively. The skewness of 0.0505 suggests a nearly symmetric distribution, while the kurtosis of −1.336 indicates a platykurtic distribution.

Figs. 5–7 present the histograms, kernel density plots, box plots, and total time on test (TTT) plots for Data I-III, respectively. These plots provide valuable insights into the distribution shapes and failure rate behaviors of the datasets. The histograms and kernel density plots reveal the distribution shapes of the datasets. Data I appears to be slightly right-skewed, while Data II seems to be slightly left-skewed. Data III's distribution is nearly symmetric. The box plots indicate the presence of outliers in the datasets. Data II has a more pronounced interquartile range (IQR) compared to Data I and Data III. The TTT plots indicate an increasing failure rate for all datasets. This suggests a wear-out failure mechanism. This observation is consistent with the Weibull distribution's ability to model increasing failure rates over time.

The datasets exhibit varying degrees of skewness and kurtosis, which can be modeled using different statistical distributions. The Weibull

Table 6
MLEs and evaluation metrics of the competitive models for Data 2.

Model	Estimate	L	AIC	CAIC	BIC	HQIC
BP-Weibull	$\hat{b} = 1.4296$ $\hat{\theta} = 2.6720$ $\hat{\alpha} = 0.7886$ $\hat{\beta} = 0.2741$ $\hat{\lambda} = 2.1638$	**251.4624**	**−492.9249**	**−488.9249**	**−487.7023**	**−491.7914**
Weibull	$\hat{b} = 0.07239$ $\hat{\theta} = 3.92467$	−11.4757	26.9514	27.6181	29.0404	27.4048
M-Weibull	$\hat{b} = 1.4539$ $\hat{\theta} = 0.4533$ $\hat{\nu} = 1.4132$	−8.2119	22.4238	23.8355	25.5573	23.1038
MO-Weibull	$\hat{b} = 1.6584$ $\hat{\theta} = 0.6235$ $\hat{\omega} = 1.9938$	−19.4023	44.8045	46.2163	47.9381	45.4846
E-Weibull	$\hat{b} = 1.8830$ $\hat{\theta} = 0.6559$ $\hat{v} = 1.8495$	−17.5463	41.0925	42.5043	44.2261	41.7726
MOD-Weibull	$\hat{b} = 0.0467$ $\hat{\theta} = 0.1983$ $\hat{\delta} = 1.9919$	−22.8524	51.7047	53.1165	54.8383	52.3848

Table 7
MLEs and evaluation metrics of the competitive models for Data 3.

Model	Estimate	L	AIC	CAIC	BIC	HQIC
BP-Weibull	$\hat{b} = 2.6154$ $\hat{\theta} = 2.1911$ $\hat{\alpha} = 0.3157$ $\hat{\beta} = 0.1568$ $\hat{\lambda} = 1.5503$	**322.8059**	**−635.6119**	**−631.6119**	**−630.3893**	**−634.4784**
Weibull	$\hat{b} = 0.0550$ $\hat{\theta} = 4.6583$	−9.0574	22.1148	22.7815	24.2039	22.5682
M-Weibull	$\hat{b} = 0.9884$ $\hat{\theta} = 0.4031$ $\hat{\nu} = 1.3836$	−8.3232	22.6464	24.0582	25.7800	23.3265
MO-Weibull	$\hat{b} = 1.6036$ $\hat{\theta} = 0.6295$ $\hat{\omega} = 1.8872$	−18.9040	43.8080	45.2198	46.9416	44.4881
E-Weibull	$\hat{b} = 1.4605$ $\hat{\theta} = 0.6235$ $\hat{v} = 1.8787$	−17.6532	41.3064	42.7182	44.4400	41.9865
MOD-Weibull	$\hat{b} = 0.0467$ $\hat{\theta} = 0.1983$ $\hat{\delta} = 1.9919$	−22.0110	50.0220	51.4337	53.1555	50.7020

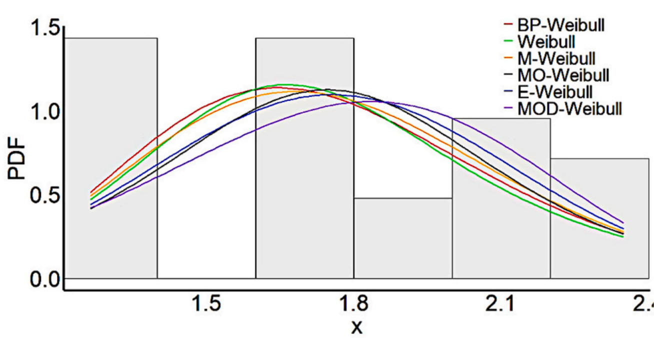

Fig. 8. Comparison evaluation metrics for candidate models under Data I.

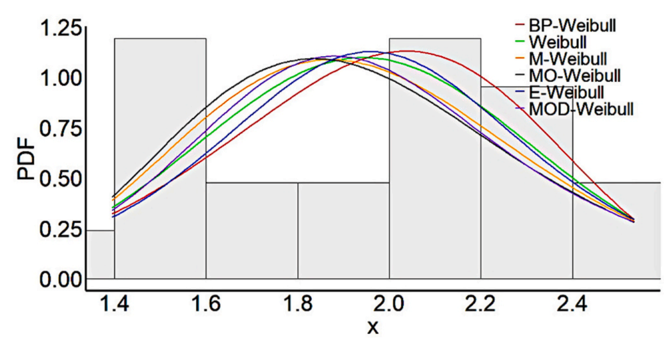

Fig. 9. Comparison evaluation metrics for candidate models under Data II.

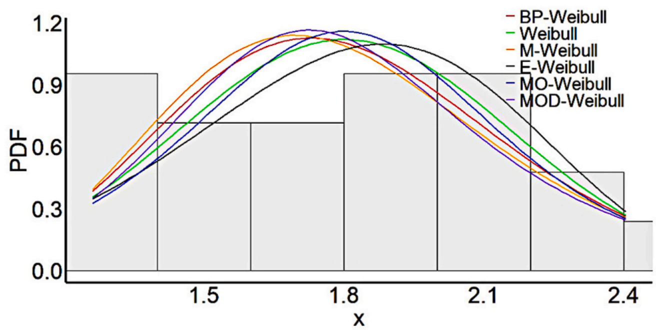

Fig. 10. Comparison evaluation metrics for candidate models under Data III.

distribution is a versatile model that can capture a wide range of failure rate behaviors. However, the unique characteristics of the radiation data, such as the platykurtic distributions and increasing failure rates, may require a more specialized model such as the proposed NBP-Weibull distribution. This new model can potentially provide a better fit to the data and offer more accurate predictions.

7.3. Performance evaluation for NBP-weibull and its competing models

This section demonstrates the flexibility and suitability of the proposed NBP-Weibull model in modeling three different radiation datasets. The performance of the NBP-Weibull model is benchmarked against several established models, including the classical Weibull model, the BP-Weibull distribution, the Maxwell-Weibull (M-Weibull) defined by Ishaq and Abiodun (Ishaq & Abiodun, 2020), the Marshall Olkin-Weibull (MO-Weibull) proposed by Ghitany et al. (Ghitany et al., 2007), the exponentiated-Weibull (E-Weibull) proposed by Nassar and Eissa (Nassar & Eissa, 2003), and the modified-Weibull (MOD-Weibull) introduced by Lai et al. (Lai et al., 2003). The selected competing models represent widely used and flexible distributions in reliability and survival analysis. These models were chosen to provide a balanced comparison between classical and generalized distributions.

Tables 5–7 provide the maximum likelihood estimates (MLEs) for the model parameters and the numerical values of evaluation metrics for all competing models across the three datasets. These metrics include AIC, BIC, HQIC, and CAIC, as well as the log-likelihood (L).

The results in Tables 5–7 indicate that the NBP-Weibull model consistently outperforms the competing models across all three datasets. It has the lowest values for AIC, HQIC, CAIC, and BIC, and the highest log-likelihood values, making it the best fit for the data. This indicates that the additional parameters in the NBP-Weibull model provide a significant improvement in fit. This demonstrates the NBP-Weibull model's ability to capture complex patterns, such as skewness and kurtosis, commonly observed in radiation data. This suggests that the NBP-Weibull model is a versatile and reliable model for analyzing radiation data.

Although the NBP-Weibull model includes multiple parameters, potential overfitting is mitigated through the use of penalized information criteria such as AIC, BIC, and CAIC. These criteria balance model fit with complexity, which ensures that additional parameters are only retained when they provide significant improvement in performance.

The plots in Figs. 8–10 show performance evaluation metrics (AIC, BIC, CAIC, and HQIC) for candidate models under Data I-II. Lower values across the criteria indicate better model performance, with the marked bar showing the best-fitting model.

Hence, the results demonstrate the adequacy of the NBP-Weibull model for modeling radiation data and its potential for accurate predictions and insights in this field. The improved performance of the NBP-Weibull model is attributed to its ability to capture both skewness and varying hazard rate behaviors simultaneously. This provides a more accurate representation of radiation-induced variability compared to traditional models.

8. Conclusion

This paper introduces the New Beta Prime-Generalized (NBP-G) family of distributions. A member of this family, the New Beta Prime-Weibull (NBP-Weibull) distribution, is proposed. The NBP-Weibull distribution is very flexible. It can model various shapes, from sharply right-skewed to near-symmetric forms. Additionally, the NBP-Weibull model accommodates various types of increasing hazard rate patterns. This makes it crucial for robust reliability and risk assessment applications in radiation engineering. Key statistical properties of the NBP-G family are derived, including moments, moment-generating function, Rényi and Tsallis entropies, stress-strength function, and order statistics. The parameters of the NBP-Weibull are derived based on the maximum likelihood method. A Monte Carlo simulation study is conducted to evaluate the performance of the MLE method. To evaluate the potential and usefulness of the NPB-Weibull model in real-world situations, we demonstrated its applicability in modeling three different radiation datasets. The results indicate that the proposed model provides an improved fit under the selected evaluation criteria when compared to the competing models. This makes it useful for reliability and risk assessment in radiation engineering. Future research can focus on developing novel regression models, exploring Bayesian parameter estimation techniques, and extending the model to accommodate more complex data structures.

CRediT authorship contribution statement

Ahmad Abubakar Suleiman: Writing – original draft, Software, Resources, Methodology, Conceptualization. **Zahrah Fayez Althobaiti:** Validation, Project administration, Funding acquisition, Formal analysis. **Hanita Daud:** Visualization, Supervision, Methodology, Funding acquisition, Conceptualization. **Nazreen Waeleh:** Visualization, Software, Resources, Funding acquisition. **Maysaa Elmahi Abd Elwahab:** Writing – original draft, Software, Funding acquisition, Data curation. **Raga Idress:** Writing – original draft, Validation, Project administration, Data curation.

Funding statement

Universiti Teknikal Malaysia Melaka (UTeM). The authors express their gratitude to Princess Nourah bint Abdulrahman University Researchers Supporting Project number (PNURSP2026R913), Princess Nourah bint Abdulrahman University, Riyadh, Saudi Arabia.

Conflicts of interest

The authors declare that they have no conflicts of interest to report regarding the present study.

Acknowledgments

This paper is funded by Universiti Teknikal Malaysia Melaka (UTeM). The authors express their gratitude to Princess Nourah bint Abdulrahman University Researchers Supporting Project number (PNURSP2026R913), Princess Nourah bint Abdulrahman University, Riyadh, Saudi Arabia. Also, the authors thank Universiti Teknologi PETRONAS, Malaysia for supporting this research.

Data availability

The data that support the findings of this study are available on request from the corresponding author.

References

Abd Elgawad, M. A., et al. (2025). A hybrid log-logistic-weibull regression model for survival analysis in leukemia patients and radiation data. *Journal of Radiation Research and Applied Sciences, 18*(3), Article 101836.

Abdelfattah, N. A., & Sayed, R. (2022). Comparative efficacy of gamma and microwave radiation in protecting peppermint from infestation by drugstore beetle (Stegobium paniceum) L. *International Journal of Tropical Insect Science, 42*(2), 1367–1372.

Adepoju, A. A., et al. (2025). A flexible extension of the log-logistic distribution with application to cancer data. *International Journal, 14*, 627.

Ahmed, A., Seyam, E. A., El-Saeed, A. R., Abdalla, E. O., Naserelden, S., & Nassr, S. G. (2026). A generalized lifetime model based on ailamujia distribution: Statistical properties, different inference estimation and applications to several fields. *Scientific African*, Article e03179.

Al-Nefaie, A. H. (2023). Applications to bio-medical data and statistical inference for a kavya-Manoharan log-logistic model. *Journal of Radiation Research and Applied Sciences, 16*(1), Article 100523. https://doi.org/10.1016/j.jrras.2023.100523

Alsaab, N. (2024). Estimation and some statistical properties of the hybrid Weibull inverse Burr type X distribution with application to cancer patient data. *Iraqi Statisticians journal*, 8–29.

Alsulami, D., & Alghamdi, A. S. (2025). A new extended weibull distribution: Estimation methods and applications in engineering, physics, and medicine. *Mathematics, 13* (20), 3262.

Althobaiti, Z. F., Aldawsari, A. M., Wiratchotisatian, P., Ishaq, A. I., & Suleiman, A. A. (2025). A novel fréchet distribution for inflation rate modeling and comparative machine learning forecasting. *Journal of Mathematics, 2025*(1), Article 5570060.

AlTwijri, M. I., Alshahrani, N. D., Elgarhy, M., Elsehetry, M., & Elkalzah, B. (2026). A new three-parameter statistical distribution with applications to biomedical and radiation data. *Journal of Radiation Research and Applied Sciences, 19*(1), Article 102167.

Alzaatreh, A., Lee, C., & Famoye, F. (2013). A new method for generating families of continuous distributions. *Metron, 71*(1), 63–79.

Arfken, G. B., & Weber, H. J. (2005). In G. B. Arfken, & H. J. Weber (Eds.) (6th ed.) *Mathematical methods for physicistsMathematical methods for physicists 6th ed.* Amsterdam; Boston: Elsevier. *Published*.

Basu, S., & Ng, H. K. T. (2025). A density power divergence measure to discriminate between generalized exponential and Weibull distributions. *Statistical Papers, 66*(1), 6.

Biazatti, E. C., Cordeiro, G. M., Rodrigues, G. M., Ortega, E. M., & de Santana, L. H. (2022). A Weibull-beta prime distribution to model COVID-19 data with the presence of covariates and censored data. *Stats, 5*(4), 1159–1173.

Çolak, A. B., Sindhu, T. N., Lone, S. A., Shafiq, A., & Abushal, T. A. (2023). Reliability study of generalized Rayleigh distribution based on inverse power law using artificial neural network with Bayesian regularization. *Tribology International, 185*, Article 108544.

Cordeiro, G. M., & De Castro, M. (2011). A new family of generalized distributions. *Journal of Statistical Computation and Simulation, 81*(7), 883–898.

Cordeiro, G. M., & Nadarajah, S. (2011). *Closed-form expressions for moments of a class of beta generalized distributions*.

Elgarhy, M., Hamdani, H., Sapkota, L. P., & Gemeay, A. M. (2025). A novel of bounded zeghdoudi distribution: Estimations, simulation and applications. *Mesopotamian Journal of CyberSecurity, 5*(3), 1292–1323.

Eugene, N., Lee, C., & Famoye, F. (2002). Beta-normal distribution and its applications. *Communications in Statistics - Theory and Methods, 31*(4), 497–512.

Feng, L., Elgawad, M. A. A., Zhu, G., & Yagoub, R. Y. (2026). A new statistical estimator with theoretical foundation and Monte Carlo simulation: Its applications in safety management and radiation sciences. *Journal of Radiation Research and Applied Sciences, 19*(1), Article 102219. https://doi.org/10.1016/j.jrras.2026.102219, 2026/03/01/.

Gasper, L., Gadde, S. R., & Kirigiti, P. J. (2025). Modelling medical data using the cosine generalized exponential distribution. *Array*, Article 100558.

Ghitany, M., Al-Awadhi, F., & Alkhalfan, L. (2007). Marshall–Olkin extended Lomax distribution and its application to censored data. *Communications in Statistics - Theory and Methods, 36*(10), 1855–1866.

Gillariose, J., Abdelwahab, M. M., Joseph, J., & Hasaballah, M. M. (2025). A gauss hypergeometric-type model for heavy-tailed survival times in biomedical research. *Symmetry, 17*(11), 1795.

Gong, Q., Zhang, Z., Zeng, L., & Ren, H. (2025). A novel extended inverse Weibull distribution: Statistical analysis and application. *PLoS One, 20*(10), Article e0335555.

Gradshteyn, I., & Ryzhik, I. (1980). *Tables of integrals, series and products*. New York: Academic Press.

Hashem, A. F., Abdelkawy, M., Muse, A. H., & Yousof, H. M. (2024). A novel generalized Weibull Poisson G class of continuous probabilistic distributions with some copulas, properties and applications to real-life datasets. *Scientific Reports, 14*(1), 1741.

Huang, Y., & Ali, S. E. O. (2026). A new heavy-tailed distribution: Its heavy-tailed characteristics with implementations in the radiation and music engineering. *Journal of Radiation Research and Applied Sciences, 19*(1), Article 102104.

Huo, W., Zhu, Z., Althobaiti, Z. F., Mohammed, A. S., Aljohani, H. M., & Elnazer, A. A. (2026). A new Log-Lévy distribution with exponent parameter: Theory, properties, and utilization in the fields of accounting and radiation industries. *Journal of Radiation Research and Applied Sciences, 19*(1), Article 102168. https://doi.org/10.1016/j.jrras.2026.102168

Imran, M., et al. (2024). The development of an extended Weibull model with applications to medicine, industry and actuarial sciences. *Scientific Reports, 14*(1), Article 12338.

Ishaq, A. I., & Abiodun, A. A. (2020). The Maxwell–Weibull distribution in modeling lifetime datasets. *Annals of Data Science, 7*(4), 639–662.

Ishaq, A., Abiodun, A., Suleiman, A., Usman, A., Mohammed, A., & Tasiu, M. (2023). Modelling Nigerian inflation rates from January 2003 to June 2023 using newly developed inverse power Chi-Square distribution. In *2023 4th international conference on data analytics for business and industry (ICDABI)* (pp. 644–651). IEEE.

Ishaq, A. I., et al. (2025). A new Log-Lomax distribution, properties, stock price, and heart attack predictions using machine learning techniques. *AIMS Mathematics, 10* (5), 12761–12807.

Jones, M. C. (2004). Families of distributions arising from distributions of order statistics. *Test, 13*(1), 1–43.

Kamal, M., Alsolmi, M. M., Mutairi, A. A., Hussam, E., Mustafa, M. S., & Nassr, S. G. (2023). A new distributional approach: Estimation, Monte Carlo simulation and applications to the biomedical data sets. *Networks and Heterogeneous Media, 18*(4).

Khan, M., & Ruidas, M. K. (2025). The mgamma distribution: Statistical properties and application to real-life data. *European Journal of Pure and Applied Mathematics, 18*(4), 6653-6653.

Klakattawi, H. S. (2022). Survival analysis of cancer patients using a new extended Weibull distribution. *PLoS One, 17*(2), Article e0264229.

Kreyszig, E. (2007). *Advanced engineering mathematics 9th edition with Wiley plus set*. John Wiley & Sons US.

Lai, C., Xie, M., & Murthy, D. (2003). A modified Weibull distribution. *IEEE Transactions on Reliability, 52*(1), 33–37.

Liu, S., Almongy, H. M., Alshahrani, N. D., & Elgarhy, M. (2026). Classical and Bayesian inference for the truncated Ailamujia distribution: Its applications in environmental Art and radiation fields. *Journal of Radiation Research and Applied Sciences, 19*(1), Article 102218. https://doi.org/10.1016/j.jrras.2026.102218

Lu, G., Salem, S., Ahmad, Z., Alsahangiti, A. M., Yusuf, M., & Bakr, M. (2023). A new tangent-based probabilistic approach with applications in sports and medical sciences. *Alexandria Engineering Journal, 81*, 560–579.

Luo, S., & Luo, S. (2026). A new estimator under the simple random sampling framework with statistical properties: Its applications in physical education and radiation. *Journal of Radiation Research and Applied Sciences, 19*(1), Article 102223. https://doi.org/10.1016/j.jrras.2026.102223

Nassar, M. M., & Eissa, F. H. (2003). On the exponentiated Weibull distribution. *Communications in Statistics - Theory and Methods, 32*(7), 1317–1336.

Noori, N. A., Elnazer, A. A., Khaleel, M. A., Elgarhy, M., & Almetwally, E. M. (2025). Enhancing neutrosophic Weibull-G family: Simulation and applications on neutrosophic data. *Journal of Cultural Analysis and Social Change*, 1899–1915.

Osi, A. A., Abdalla, G. S. S., Sawaran Singh, N. S., & Suleiman, A. A. (2025). Advancing lifetime data modeling via the Marshall-Olkin cosine Topp-Leone distribution family. *Computational Journal of Mathematical and Statistical Sciences, 4*(2), 476–499.

Panitanarak, U., et al. (2025a). "A new beta distribution with interdisciplinary data analysis. *AIMS Math, 10*, 8495–8527.

Panitanarak, U., Ishaq, A. I., Abiodun, A. A., Daud, H., & Suleiman, A. A. (2025). A new Maxwell-Log logistic distribution and its applications for mortality rate data. *Journal of the Nigerian Society of Physical Sciences*, 1976-1976.

Rahmouni, M., & Ziedan, D. (2025). The Weibull-generalized shifted geometric distribution: Properties, estimation, and applications. *AIMS MATHEMATICS, 10*(4), 9773–9804.

Semary, H., et al. (2025a). Advancing survival regression using the NGOF exponentiated Weibull distribution for vesicovaginal fistula and radiation data applications. *Journal of Radiation Research and Applied Sciences, 18*(2), Article 101497.

Semary, H., et al. (2025b). A new modified Sine-Weibull distribution for modeling medical data with dynamic structures. *Journal of Radiation Research and Applied Sciences, 18*(2), Article 101427.

Stewart, J., Clegg, D., & Watson, S. (2021). *Calculus: Early transcendentals*. Cengage.

Suleiman, A. A., Daud, H., Singh, N. S. S., Othman, M., Ishaq, A. I., & Sokkalingam, R. (2023). A novel odd beta prime-logistic distribution: Desirable mathematical properties and applications to engineering and environmental data. *Sustainability, 15* (13), Article 10239.

Suleiman, A. A., Daud, H., Usman, A. G., Abba, S. I., Othman, M., & Elgarhy, M. (2025c). A new two-parameter half-logistic distribution with numerical analysis and applications. *Journal of Statistical Sciences and Computational Intelligence, 1*(1), 1–28.

Suleiman, A. A., et al. (2025a). An extension of the gompertz distribution for modeling COVID-19 mortality dynamics. *International Journal of Analysis and Applications, 23*, 206-206.

Suleiman, A. A., et al. (2025b). The modified gamma distribution and machine learning for modeling and classification of groundwater potability. *Mathematical Modelling of Engineering Problems, 12*(10).

Suleiman, A. A., et al. (2025d). A new statistical model for advanced modeling of cancer disease data. *Kuwait Journal of Science*, Article 100429.

Sun, M., Metwally, D. S., Kayid, M., & El-Qurashi, M. A. (2026). A new statistical method with Monte Carlo simulation: It's applications in the vocal education and radiation sector. *Journal of Radiation Research and Applied Sciences, 19*(1), Article 102200. https://doi.org/10.1016/j.jrras.2026.102200

Tu, X., et al. (2025). A new trigonometric-inspired probability distribution: A simulation study and applications in reliability and hydrology. *Alexandria Engineering Journal, 113*, 181–194.

Tung, Y. L., Abdalla, G. S. S., Abd El-Raouf, M., & El-Qurashi, M. (2026). A modified sine Weibull distribution with applications to finance and radiation sectors. *Journal of Radiation Research and Applied Sciences, 19*(1), Article 102088.

Wu, X., et al. (2023). A new Cosine-Weibull model: Distributional properties with applications to basketball and medical sectors. *Alexandria Engineering Journal, 66*, 751–767.

Yu, Y., et al. (2024). Adopting a new sine-induced statistical model and deep learning methods for the empirical exploration of the music and reliability data. *Alexandria Engineering Journal, 104*, 396–408.

Zhang, X., Almongy, H. M., Alshahrani, N. D., & Elgarhy, M. (2026). The problem of generalized estimation methods of population distribution functions with auxiliary information: The international trade and radiation measurements. *Journal of Radiation Research and Applied Sciences, 19*(1), Article 102107.